

Supplementary Information

**Hydrogenation/Dehydrogenation of N-Heterocycles Catalyzed by Ruthenium
Complexes Based on Multimodal Proton-responsive CNN(H) Pincer Ligands**

Práxedes Sánchez,^a Martín Hernández-Juárez,^b Nuria Rendón,^{*a} Joaquín López-Serrano,^a
Laura L. Santos,^a Eleuterio Álvarez,^a Margarita Paneque^a and Andrés Suárez^{*a}

^a *Instituto de Investigaciones Químicas (IIQ), Departamento de Química Inorgánica and Centro de Innovación en Química Avanzada (ORFEO-CINQA). CSIC and Universidad de Sevilla.*

^b *Área Académica de Química. Centro de Investigaciones Químicas. Universidad Autónoma del Estado de Hidalgo. Km. 14.5 Carretera Pachuca-Tulancingo, Ciudad del Conocimiento, C.P. 42184, Mineral de la Reforma, Hidalgo, Mexico.*

E-mail: nuria@iiq.csic.es; andres.suarez@iiq.csic.es

Table of Contents

1. Synthetic procedures and analytical data.....	3
1.1. General procedures.....	3
1.2. Synthesis of imidazolium salts 1a-c	3
1.3. Synthesis of silver complexes 2a-c	5
1.4. Synthesis of ruthenium complexes 3a-c	6
1.5. Synthesis of complexes 6-8	8
1.6. Catalytic reactions.....	10
2. Reactions of complexes 6, 7 and 8 with D₂.....	12
3. NMR spectroscopy monitoring of hydrogenation reactions.....	14
4. X-Ray structure analysis of complexes 3a and 3b.....	19
5. DFT calculations.....	23
6. Selected NMR spectra of complexes 2-8.....	24
6.1. Selected NMR spectra for complexes 2a-c	24
6.2. Selected NMR spectra for complexes 3a-c	27
6.3. Selected NMR spectra for complex 6	30
6.4. Selected NMR spectra for complex 7	32
6.5. Selected NMR spectra for complex 8	34
7. NMR spectra of catalytic dehydrogenation reactions.....	36

1. Synthetic procedures and analytical data

1.1. General procedures

All reactions and manipulations were performed under nitrogen or argon, either in a MBraun Unilab Pro glovebox or using standard Schlenk-type techniques. All solvents were dried and distilled under nitrogen, using the following desiccants: sodium-benzophenone-ketyl for diethyl ether (Et₂O) and tetrahydrofuran (THF); sodium for pentane and toluene; CaH₂ for dichloromethane and acetonitrile (CH₂Cl₂, CH₃CN). [2-Bromomethyl-6-(3-mesitylimidazolium-1-yl)methyl]pyridine bromide¹ and [RuHCl(CO)(PPh₃)₃]² were prepared as previously described. All other reagents were purchased from commercial suppliers and used as received. NMR spectra were obtained on Bruker DPX-300, DRX-400, AVANCEIII/ASCEND 400R or DRX-500 spectrometers. ³¹P{¹H} NMR shifts were referenced to external 85% H₃PO₄, while ¹³C{¹H} and ¹H shifts were referenced to the residual signals of deuterated solvents. All data are reported in ppm downfield from Me₄Si. All NMR measurements were carried out at 25 °C. NMR signal assignments were confirmed by 2D NMR spectroscopy (¹H-¹H COSY, ¹H-¹H NOESY, ¹H-¹³C HSQC and ¹H-¹³C HMBC) for all the complexes. The following NMR abbreviations have been used: s, singlet; d, doublet; dd, doublet of doublets; ddd, doublet of doublets of doublets; t, triplet; m, multiplet; br, broad signal; C_q, quaternary carbon.

HRMS data were obtained on a JEOL JMS-SX 102A mass spectrometer at the Instrumental Services of Universidad de Sevilla (CITIUS). Elemental analyses were run by the Analytical Service of the Instituto de Investigaciones Químicas in a Leco TrueSpec Micro elemental analyzer. IR spectra were acquired on a Bruker Tensor 27 instrument.

1.2. Synthesis of imidazolium salts 1a-c

Compound 1a: ^tBuNH₂ (0.656 g, 8.98 mmol) was added to a solution of [2-bromomethyl-6-(3-mesitylimidazolium-1-yl)methyl]pyridine bromide (0.810 g, 1.80 mmol) in CH₃CN (25 mL). The resulting mixture was stirred overnight, and filtered. Volatiles were removed under vacuum, and the residue was washed with Et₂O (3 × 10 mL). The resulting solid was dissolved in CH₂Cl₂ (15 mL) and treated with phenethyldiethylamine ScavengePore resin (0.66 mmol/g loading; 3.50 g) for 1 h. The resin was filtered off, and the procedure was repeated twice. The solid obtained after solvent evaporation was washed with Et₂O (3 × 10

¹ P. Sánchez, M. Hernández-Juárez, E. Álvarez, M. Paneque, N. Rendón and A. Suárez, *Dalton Trans.* 2016, **45**, 16997

² N. Ahmad, J. J. Levison, S. D. Robinson, M. F. Uttley, E. R. Wonchoba, G. W. Parshall, in *Inorg. Synth. Vol. 15* (Ed.: G. W. Parshall), Wiley, Hoboken, 1974, pp. 45–64.

mL) to give a white solid (0.742 g, 93%). ^1H NMR (500 MHz, CD_2Cl_2): δ 10.45 (s, 1H; H arom, imid), 8.27 (s, 1H; H arom, imid), 7.77 (dd, $^3J(\text{H,H}) = 7.5$ Hz, $^3J(\text{H,H}) = 7.5$ Hz, 1H; H arom, py), 7.70 (d, $^3J(\text{H,H}) = 7.5$ Hz, 1H; H arom, py), 7.53 (d, $^3J(\text{H,H}) = 7.5$ Hz, 1H; H arom, py), 7.20 (s, 1H; H arom, imid), 7.08 (s, 2H; 2 H arom, mes), 5.97 (s, 2H; imid- CH_2), 5.22 (br s, 1H; NH), 4.07 (s, 2H; CH_2NH), 2.39 (s, 3H; CH_3), 2.13 (s, 6H; 2 CH_3), 1.41 ppm (s, 9H; $\text{C}(\text{CH}_3)_3$); $^{13}\text{C}\{^1\text{H}\}$ NMR (126 MHz, CD_2Cl_2): δ 156.3 (C_q arom), 152.0 (C_q arom), 141.2 (C_q arom), 138.5 (CH arom), 138.1 (CH arom), 134.4 (2 C_q arom), 130.9 (C_q arom), 129.7 (2 CH arom), 124.1 (CH arom), 123.3 (CH arom), 122.6 (CH arom), 122.6 (CH arom), 54.9 ($\text{C}(\text{CH}_3)_3$), 53.5 (imid- CH_2), 46.9 (CH_2NH), 27.1 ($\text{C}(\text{CH}_3)_3$), 20.8 (CH_3), 17.6 ppm (2 CH_3); HRMS (ESI): m/z calcd for $\text{C}_{23}\text{H}_{31}\text{N}_4$: 363.2540 [$(M-\text{Br})^+$]; found: 363.2543.

Compound 1b: To a solution of [2-bromomethyl-6-(3-mesitylimidazolium-1-yl)methyl]pyridine bromide (0.200 g, 0.44 mmol) in CH_3CN (15 mL) was added benzylamine (0.143 g, 1.33 mmol). The resulting mixture was stirred overnight, and volatiles were removed under vacuum. The residue was extracted with CH_2Cl_2 (2×10 mL), the solvent was evaporated and the solid was washed with Et_2O (2×10 mL) and pentane (2×10 mL). White solid (0.133 g, 63%). ^1H NMR (300 MHz, CD_2Cl_2): δ 10.30 (s, 1H; H arom, imid), 8.04 (s, 1H; H arom, imid), 7.76 (dd, $^3J(\text{H,H}) = 7.5$ Hz, $^3J(\text{H,H}) = 7.5$ Hz, 1H; H arom py), 7.69 (d, $^3J(\text{H,H}) = 7.5$ Hz, 1H; H arom, py), 7.41 (d, $^3J(\text{H,H}) = 7.2$ Hz, 2H; 2 H arom), 7.37 (d, $^3J(\text{H,H}) = 7.5$ Hz, 1H; H arom, py), 7.30 (m, 3H; 3 H arom), 7.13 (s, 1H; H arom, imid), 7.04 (s, 2H; 2 H arom, mes), 5.99 (s, 2H; imid- CH_2), 3.92 (s, 2H; CH_2NH), 3.89 (s, 2H; CH_2NH), 2.64 (br s, 1H; NH), 2.36 (s, 3H; CH_3), 2.05 ppm (s, 6H; 2 CH_3); $^{13}\text{C}\{^1\text{H}\}$ NMR (101 MHz, CD_2Cl_2): δ 159.4 (C_q arom), 152.4 (C_q arom), 141.7 (C_q arom), 138.9 (C_q arom), 138.7 (CH arom), 138.4 (CH arom), 134.8 (2 C_q arom), 131.2 (C_q arom), 130.1 (2 CH arom), 129.1 (2 CH arom), 128.8 (2 CH arom), 127.7 (CH arom), 124.1 (CH arom), 123.0 (CH arom), 122.9 (CH arom), 122.4 (CH arom), 54.2 (imid- CH_2), 53.6 (CH_2NH), 53.1 (CH_2NH), 21.2 (CH_3), 17.8 ppm (2 CH_3); HRMS (ESI): m/z calcd for $\text{C}_{26}\text{H}_{29}\text{N}_4$: 397.2392 [$(M-\text{Br})^+$]; found: 397.2387.

Compound 1c: To a solution of [2-bromomethyl-6-(3-mesitylimidazolium-1-yl)methyl]pyridine bromide (0.700 g, 1.55 mmol) in CH_3CN (15 mL) was added aniline (0.433 g, 4.65 mmol). The resulting mixture was stirred overnight, and volatiles were removed under vacuum. The residue was extracted with CH_2Cl_2 (2×10 mL), the solvent was evaporated and the solid was washed with Et_2O (2×10 mL) and pentane (2×10 mL). White solid (0.650 g, 90%). ^1H NMR (400 MHz, CD_2Cl_2): δ 10.29 (s, 1H; H arom, imid), 8.02 (s, 1H; H arom, imid), 7.73 (m, 2H; 2 H arom), 7.38 (d, $^3J(\text{H,H}) = 6.7$ Hz, 1H; H arom, py),

7.14 (m, 3H; 3 H arom), 7.06 (s, 2H; 2 H arom, mes), 6.71 (m, 3H; 3 H arom), 6.07 (s, 2H; imid-CH₂), 4.85 (br, 1H; NH), 4.44 (s, 2H; CH₂NH), 2.39 (s, 3H; CH₃), 2.09 ppm (s, 6H; 2 CH₃); ¹³C{¹H} NMR (101 MHz, CD₂Cl₂): δ 159.0 (C_q arom), 152.2 (C_q arom), 147.4 (C_q arom), 141.3 (C_q arom), 138.31 (CH arom), 138.1 (CH arom), 134.4 (2 C_q arom), 130.8 (C_q arom), 129.7 (2 CH arom), 129.1 (2 CH arom), 123.8 (CH arom), 122.6 (CH arom), 122.0 (CH arom), 121.9 (CH arom), 117.9 (CH arom), 113.4 (2 CH arom), 53.4 (imid-CH₂), 49.3 (CH₂NH), 20.8 (CH₃), 17.4 ppm (2 CH₃); HRMS (ESI): *m/z* calcd. for C₂₅H₂₇N₄: 383.2230 [(M-Br)⁺]; found: 383.2224.

1.3. Synthesis of silver complexes 2a-c

Complex 2a: A solution of **1a** (0.742 g, 1.35 mmol) in CH₂Cl₂ (10 mL) was treated with Ag₂O (0.250 g, 1.08 mmol), and stirred overnight. The solution was filtered, and the solvent was removed under vacuum to give a light brown solid (0.861 g, 93%). ¹H NMR (400 MHz, CD₂Cl₂): δ 7.72 (dd, ³J(H,H) = 7.5 Hz, ³J(H,H) = 7.5 Hz, 1H; H arom, py), 7.39 (s, 1H; H arom, NHC), 7.38 (d, ³J(H,H) = 7.5 Hz, 1H; H arom, py), 7.12 (d, ³J(H,H) = 7.5 Hz, 1H; H arom, py), 7.05 (s, 1H; H arom, NHC), 7.05 (s, 2H; 2 H arom, mes), 5.53 (s, 2H; CH₂-NHC), 3.90 (br d, ³J(H,H) = 4.7 Hz, 2H; CH₂NH), 2.40 (s, 3H; CH₃), 2.04 (s, 6H; 2 CH₃), 1.65 (br, 1H; NH), 1.19 ppm (s, 9H; C(CH₃)₃); ¹³C{¹H} NMR (101 MHz, CD₂Cl₂): δ 162.1 (C_q arom), 154.9 (C_q arom), 140.0 (C_q arom), 138.0 (CH arom), 136.0 (C_q arom), 135.3 (2 C_q arom), 129.7 (2 CH arom), 123.2 (CH arom), 122.4 (CH arom), 122.2 (CH arom), 120.1 (CH arom), 57.5 (CH₂-NHC), 50.9 (C(CH₃)₃), 48.8 (CH₂NH), 29.3 (C(CH₃)₃), 21.2 (CH₃), 17.9 ppm (2 CH₃), due to significant signal broadening, the chemical shift for the C²(NHC)-Ag carbon was determined from the ¹H-¹³C HMBC experiment, appearing at 183.1 ppm; elemental analysis calcd (%) for C₂₃H₃₀AgBrN₄: C 50.20, H 5.50, N 10.18; found: C 50.43, H 5.22, N 9.82.

Complex 2b: This complex was prepared as described above for **2a**. Brown solid (0.065 g, 40%). Satisfactory elemental analysis for this compound could not be obtained. ¹H NMR (400 MHz, CD₂Cl₂): δ 7.68 (dd, ³J(H,H) = 7.6 Hz, ³J(H,H) = 7.6 Hz, 1H; H arom, py), 7.35 (m, 3H; 3 H arom), 7.30 (m, 3H; 3 H arom), 7.25 (m, 1H; H arom), 7.08 (d, ³J(H,H) = 7.6 Hz, 1H; H arom, py), 6.99 (m, 3H; 3 H arom), 5.45 (s, 2H; CH₂-NHC), 3.88 (br d, ³J(H,H) = 6.5 Hz, 2H; CH₂NH), 3.81 (br d, ³J(H,H) = 6.0 Hz, 2H; CH₂NH), 2.35 (s, 3H; CH₃), 2.15 (br m, 1H; NH), 1.95 ppm (s, 6H; 2 CH₃); ¹³C DEPT (101 MHz, CD₂Cl₂): δ 183.5 (br; C-2 NHC), 160.9 (C_q arom), 155.1 (C_q arom), 140.9 (C_q arom), 139.8 (C_q arom), 138.0 (CH arom), 135.9 (C_q arom), 135.2 (2 C_q arom), 129.6 (2 CH arom), 128.6 (2 CH arom), 128.5 (2 CH

arom), 127.2 (CH arom), 123.2 (CH arom), 122.5 (CH arom), 122.1 (CH arom), 120.3 (CH arom), 57.3 (CH₂-NHC), 54.6 (CH₂NH), 53.7 (CH₂NH), 21.2 (CH₃), 17.8 ppm (2 CH₃).

Complex 2c: This complex was prepared as described above for **2a**. Brown solid (0.195 g, 79%). ¹H NMR (400 MHz, CD₂Cl₂): δ 7.71 (dd, ³J(H,H) = 7.8 Hz, ³J(H,H) = 7.6 Hz, 1H; H arom, py), 7.40 (d, ³J(H,H) = 1.4 Hz, 1H; H arom, NHC), 7.36 (d, ³J(H,H) = 7.8 Hz, 1H; H arom, py), 7.16 (m, 3H; 3 H arom), 7.04 (m, 3H; 3 H arom), 6.70 (m, 3H; 3 H arom), 5.50 (s, 2H; CH₂-NHC), 1.01 (br t, ³J(H,H) = 5.6 Hz, 1H; NH), 4.46 (br d, ³J(H,H) = 5.6 Hz, 2H; CH₂NH), 2.40 (s, 3H; CH₃), 2.00 ppm (s, 6H; 2 CH₃); ¹³C DEPT (101 MHz, CD₂Cl₂): δ 183.6 (C-2 NHC), 159.4 (C_q arom), 155.0 (C_q arom), 148.3 (C_q arom), 139.8 (C_q arom), 138.1 (CH arom), 135.9 (C_q arom), 135.2 (2 C_q arom), 129.6 (2 CH arom), 129.5 (2 CH arom), 123.2 (CH arom), 122.5 (CH arom), 121.6 (CH arom), 120.5 (CH arom), 117.6 (CH arom), 113.2 (2 CH arom), 57.1 (CH₂-NHC), 49.2 (CH₂NH), 21.2 (CH₃), 17.8 ppm (2 CH₃); elemental analysis calcd (%) for C₂₅H₂₆AgBrN₄: C 52.65, H 4.60, N 9.82; found: C 52.32, H 4.80, N 10.17.

1.4. Synthesis of ruthenium complexes 3a-c

Complex 3a: A suspension of **2a** (0.400 g, 0.73 mmol) and RuHCl(CO)(PPh₃)₃ (0.692 g, 0.73 mmol) in THF (30 mL) was heated to 55 °C for 24 h. The resulting mixture was filtered, the volatiles evaporated, and the resulting solid was extracted with MeOH (2 × 10 mL). Solvent was removed under vacuum, and the solid was dissolved in CH₃CN (15 mL) and treated with PPh₃ (0.210 g, 0.80 mmol) and NaBF₄ (0.087 g, 0.80 mmol) overnight. The solvent was evaporated, the residue was extracted with CH₂Cl₂ (2 × 10 mL), and the complex was precipitated by slow addition of toluene, and washed with pentane (2 × 10 mL). Light brown solid (0.536 g, 88%). Crystals of **3a** suitable for X-ray diffraction analysis were grown from a saturated solution of the complex in CH₂Cl₂. ¹H NMR (400 MHz, CD₂Cl₂): δ 7.83 (dd, ³J(H,H) = 7.7 Hz, ³J(H,H) = 7.7 Hz, 1H; H arom, py), 7.42 (m, 5H; 3 H arom, PPh₃ + 2 H arom, py), 7.38 (d, ³J(H,H) = 1.9 Hz, 1H; H arom, NHC), 7.31 (ddd, ³J(H,H) = 7.4 Hz, ³J(H,H) = 7.4 Hz, ⁴J(H,P) = 1.2 Hz, 6H; 6 H arom, PPh₃), 7.13 (dd, ³J(H,H) = 8.5 Hz, ³J(H,P) = 8.5 Hz, 6H; 6 H arom, PPh₃), 7.02 (s, 1H; H arom, mes), 7.06 (s, 1H; H arom, mes), 6.93 (d, ³J(H,H) = 1.9 Hz, 1H; H arom, NHC), 5.00 (d, ²J(H,H) = 15.6 Hz, 1H; CHH-NHC), 4.21 (d, ²J(H,H) = 15.6 Hz, 1H; CHH-NHC), 4.18 (dd, ²J(H,H) = 14.7 Hz, ³J(H,H) = 3.7 Hz, 1H; CHHN), 3.95 (dd, ²J(H,H) = 14.2 Hz, ³J(H,H) = 13.6 Hz, 1H; CHHN), 2.71 (br ddd, ³J(H,H) = 12.2 Hz, ³J(H,H) = 3.4 Hz, ³J(H,P) = 3.4 Hz, 1H; NH), 2.40 (s, 3H; CH₃), 2.21 (s, 3H; CH₃), 2.04 (s, 3H; CH₃), 0.98 (s, 9H; C(CH₃)₃), -7.79 ppm (d, ²J(H,P) = 114.0 Hz, 1H; RuH); ³¹P{¹H} NMR (121 MHz, CD₂Cl₂): δ 22.5 ppm; ¹³C{¹H} NMR (101 MHz, CD₂Cl₂): δ 208.3 (d,

$J(\text{C,P}) = 6 \text{ Hz}$; CO), 185.2 (d, $J(\text{C,P}) = 5 \text{ Hz}$; C2-NHC), 161.1 (C_q arom), 154.3 (C_q arom), 139.7 (C_q arom), 139.0 (CH arom), 137.2 (C_q arom), 136.6 (C_q arom), 134.6 (d, $J(\text{C,P}) = 27 \text{ Hz}$; 3 C_q arom), 134.5 (C_q arom), 132.9 (d, $J(\text{C,P}) = 11 \text{ Hz}$; 6 CH arom), 130.5 (3 CH arom), 129.6 (CH arom), 129.3 (CH arom), 129.3 (d, $J(\text{C,P}) = 8 \text{ Hz}$; 6 CH arom), 123.9 (CH arom), 123.4 (CH arom), 123.2 (CH arom), 121.8 (CH arom), 57.8 ($\text{C}(\text{CH}_3)_3$), 55.5 (CH_2NH), 54.4 ($\text{CH}_2\text{-NHC}$), 28.4 ($\text{C}(\text{CH}_3)_3$), 21.2 (CH_3), 19.3 (CH_3), 19.1 ppm (CH_3); IR (Nujol): $\nu = 1933 \text{ cm}^{-1}$ (CO); elemental analysis calcd (%) for $\text{C}_{42}\text{H}_{46}\text{BF}_4\text{N}_4\text{OPRu}$: C 59.93, H 5.51, N 6.66; found: C 59.81, H 5.27, N 6.80.

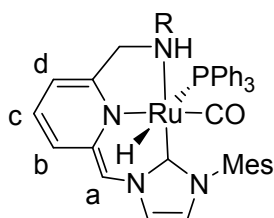
Complex 3b: This complex was prepared as described above for **3a**, with the exception that the obtained solid was recrystallized from MeOH. Light brown solid (0.121 g, 39%). Crystals of **3b** suitable for X-ray diffraction analysis were grown from a saturated solution of the complex in MeOH. ^1H NMR (400 MHz, CD_2Cl_2): δ 7.83 (dd, $^3J(\text{H,H}) = 7.7 \text{ Hz}$, $^3J_{\text{HH}} = 7.7 \text{ Hz}$, 1H; H arom, py), 7.50 (d, $^3J(\text{H,H}) = 2.0 \text{ Hz}$, 1H; H arom, NHC), 7.5 (m, 2H; 2 H arom, PPh_3), 7.40 (d, $^3J(\text{H,H}) = 7.7 \text{ Hz}$, 1H; H arom, py), 7.32 (m, 11H; 11 H arom), 7.02 (s, 1H; H arom, mes), 6.92 (m, 6H; 6 H arom), 6.88 (s, 1H; H arom, mes), 6.86 (d, $^3J(\text{H,H}) = 2.0 \text{ Hz}$, 1H; H arom, NHC), 6.62 (m, 2H; 2 H arom, CH_2Ph), 5.20 (d, $^2J(\text{H,H}) = 16.0 \text{ Hz}$, 1H; CHH-NHC), 4.34 (d, $^2J(\text{H,H}) = 16.0 \text{ Hz}$, 1H; CHH-NHC), 4.00 (m, 2H; 2 CHHNH), 3.83 (m, 2H; 2 CHHNH), 2.87 (br m, 1H; NH), 2.33 (s, 3H; CH_3), 1.97 (s, 3H; CH_3), 1.85 (s, 3H; CH_3), -7.30 ppm (d, $^2J(\text{H,P}) = 109.9 \text{ Hz}$, 1H; RuH); $^{31}\text{P}\{^1\text{H}\}$ NMR (162 MHz, CD_2Cl_2): δ 24.5 ppm; $^{13}\text{C}\{^1\text{H}\}$ NMR (101 MHz, CD_2Cl_2): δ 206.8 (d, $J(\text{C,P}) = 7 \text{ Hz}$; CO), 186.2 (d, $J(\text{C,P}) = 5 \text{ Hz}$; C-2 NHC), 159.9 (C_q arom), 154.9 (C_q arom), 139.5 (C_q arom), 139.1 (CH arom), 137.1 (C_q arom), 136.7 (C_q arom), 136.6 (C_q arom), 136.4 (C_q arom), 133.3 (d, $J(\text{C,P}) = 28 \text{ Hz}$; 3 C_q arom), 132.9 (d, $J(\text{C,P}) = 11 \text{ Hz}$; 6 CH arom), 130.8 (3 CH arom), 129.6 (m; 9 CH arom), 129.2 (CH arom), 129.1 (CH arom), 128.8 (2 CH arom), 124.9 (CH arom), 123.2 (CH arom), 123.0 (CH arom), 121.6 (CH arom), 63.0 (CH_2NH), 59.9 (CH_2NH), 54.5 ($\text{CH}_2\text{-NHC}$), 21.2 (CH_3), 19.2 (CH_3), 18.9 ppm (CH_3); IR (Nujol): $\nu = 1936 \text{ cm}^{-1}$ (CO); elemental analysis calcd (%) $\text{C}_{45}\text{H}_{44}\text{BF}_4\text{N}_4\text{OPRu}$: C 61.72, H 5.06, N 6.40; found: C 61.84, H 4.85, N 6.38.

Complex 3c: This complex was prepared as described above for **3a**, with the exception that the obtained solid was recrystallized from MeOH. Although complex **3c** is stable under inert atmosphere in the solid state, it gradually decomposes in solution. Hence, spectroscopically pure samples could not be obtained. Signals of the complex in the ^1H and $^{13}\text{C}\{^1\text{H}\}$ NMR spectra were assigned with the help of $^1\text{H},^{13}\text{C}$ -HMQC and $^1\text{H},^{13}\text{C}$ -HMBC experiments. Light brown solid (0.104 g, 35%). ^1H NMR (400 MHz, CD_2Cl_2): δ 7.92 (dd, $^3J(\text{H,H}) = 7.7 \text{ Hz}$, $^3J(\text{H,H}) = 7.7 \text{ Hz}$, 1H; H arom, py), 7.51 (m, 2H; 2 H arom), 7.42 (m, 4H; 4

H arom), 7.24 (m, 8H; 8 H arom), 7.02 (s, 1H; H arom), 6.82 (m, 10H; 10 H arom), 6.76 (s, 1H; H arom), 5.15 (d, $^2J(\text{H,H}) = 15.6$ Hz, 1H; CHH-NHC), 4.54 (m, 3H; 2 CHHNH + NH), 4.40 (d, $^2J(\text{H,H}) = 15.6$ Hz, 1H; CHHN-NHC), 2.29 (s, 3H; CH₃), 2.04 (s, 3H; CH₃), 1.78 (s, 3H; CH₃), -7.05 ppm (d, $^2J(\text{H,P}) = 110.7$ Hz, 1H; RuH); $^{31}\text{P}\{^1\text{H}\}$ NMR (162 MHz, CD₂Cl₂): δ 23.6 ppm; $^{13}\text{C}\{^1\text{H}\}$ NMR (101 MHz, CD₂Cl₂): δ 205.6 (d, $J(\text{C,P}) = 7$ Hz; CO), 185.8 (d, $J(\text{C,P}) = 4$ Hz; C-2 NHC), 159.6 (C_q arom), 154.7 (C_q arom), 147.1 (C_q arom), 139.6 (C_q arom), 139.2 (CH arom), 137.0 (C_q arom), 136.6 (C_q arom), 136.4 (C_q arom), 133.6 (d, $J(\text{C,P}) = 29$ Hz; 3 C_q arom), 133.2 (d, $J(\text{C,P}) = 12$ Hz; 6 CH arom), 130.7 (3 CH arom), 129.5 (m; 9 CH arom), 129.1 (CH arom), 126.7 (CH arom), 124.7 (CH arom), 123.3 (CH arom), 123.1 (CH arom), 122.8 (2 CH arom), 122.0 (CH arom), 65.6 (CH₂NH), 54.6 (CH₂-NHC), 21.1 (CH₃), 19.1 (CH₃), 18.8 ppm (CH₃); IR (Nujol): $\nu = 1958$ cm⁻¹ (CO); HRMS (ESI): m/z calcd. for C₄₄H₄₂N₄OP¹⁰²Ru: 775.2140 [(M-BF₄)⁺]; found: 775.2133.

1.5. Synthesis of complexes 6-8

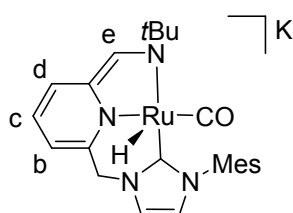
Complex 6: In a J.Young valved NMR tube, THF-*d*₈ (0.5 mL) was added to a mixture of **3a** (0.023 g, 0.027 mmol) and KO^tBu (0.004 g, 0.035 mmol), giving rise to the immediate formation of a dark red solution. The resulting sample was analyzed by NMR spectroscopy. Attempted isolation of complex **6** was unsuccessful due to significant decomposition during work-up.



^1H NMR (400 MHz, THF-*d*₈): δ 7.32 (m, 15H; 15 H arom, PPh₃), 6.94 (s, 1H; H arom, mes), 6.81 (s, 1H; H arom, mes), 6.75 (d, $^3J(\text{H,H}) = 1.9$ Hz, 1H; H arom, NHC), 6.65 (d, $^3J(\text{H,H}) = 1.9$ Hz, 1H; H arom, NHC), 6.09 (dd, $^3J(\text{H,H}) = 9.0$ Hz, $^3J_{\text{HH}} = 6.1$ Hz, 1H; H^c), 5.14 (d, $^3J(\text{H,H}) = 6.0$ Hz, 1H; H^d), 5.08 (d, $^3J(\text{H,H}) = 9.0$ Hz, 1H; H^b), 4.38 (s, 1H; H^a), 3.43 (dd, $^2J(\text{H,H}) = 12.0$ Hz, $^3J(\text{H,H}) = 12.0$ Hz, 1H; CHHNH), 3.09 (dd, $^2J(\text{H,H}) = 11.2$ Hz, $^3J_{\text{HH}} = 1.9$ Hz, 1H; CHHNH), 2.31 (s, 3H; CH₃), 2.12 (s, 3H; CH₃), 1.76 (overlapped with solvent signal; NH), 1.73 (s, 3H; CH₃), 0.93 (s, 9H; C(CH₃)₃), -7.64 ppm (d, $^2J(\text{H,P}) = 140.2$ Hz, 1H; RuH); $^{31}\text{P}\{^1\text{H}\}$ NMR (121 MHz, THF-*d*₈): δ 16.0 ppm; $^{13}\text{C}\{^1\text{H}\}$ NMR (101 MHz, THF-*d*₈): δ 210.2 (CO), 177.3 (C-2 NHC), 155.7 (C_q arom), 143.0 (C_q arom), 137.9 (C_q arom), 137.7 (C_q arom), 137.6 (C_q arom), 137.4 (C_q arom), 133.6 (d, $J(\text{C,P}) = 16$ Hz; 6 CH arom), 129.0 (m; C^c + 10 CH arom + 3 C_q arom), 120.8 (2 CH arom), 120.0 (CH arom), 111.8 (C^b), 96.8 (C^d),

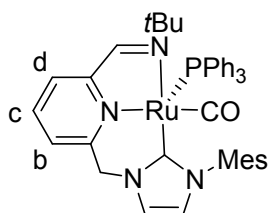
90.9 (C^a), 55.6 (C(CH₃)₃), 54.7 (CH₂NH), 28.4 (C(CH₃)₃), 21.1 (CH₃), 19.2 (CH₃), 18.7 ppm (CH₃).

Complex 7: In a J.Young valved NMR tube, THF-*d*₈ (0.5 mL) was added to a mixture of **3a** (0.025 g, 0.030 mmol) and KHMDS (0.018 g, 0.090 mmol) giving rise initially to a dark red solution that gradually evolves to dark violet. The resulting solution was analyzed by NMR spectroscopy after 24 h. Attempted isolation of complex **7** was unsuccessful due to significant decomposition during work-up.



¹H NMR (400 MHz, THF-*d*₈): δ 7.05 (d, ³J(H,H) = 2.0 Hz, 1H; H arom, NHC), 6.80 (s, 1H; H arom, mes), 6.74 (s, 1H; H arom, mes), 6.69 (s, 1H; H^e), 6.59 (d, ³J(H,H) = 2.0 Hz, 1H; H arom, NHC), 6.54 (d, ³J(H,H) = 8.9 Hz, 1H; H^b), 5.83 (dd, ³J(H,H) = 8.9 Hz, ³J_{HH} = 5.7 Hz, 1H; H^c), 5.33 (d, ³J(H,H) = 5.7 Hz, 1H; H^d), 4.83 (d, ²J(H,H) = 12.7 Hz, 1H; H^a), 4.56 (d, ²J(H,H) = 12.7 Hz, 1H; H^a), 2.26 (s, 3H; CH₃), 2.02 (s, 3H; CH₃), 1.57 (s, 3H; CH₃), 1.50 (s, 9H; C(CH₃)₃), -17.09 ppm (s, 1H; RuH); ³¹P{¹H} NMR (121 MHz, THF-*d*₈): δ -7.3 ppm (free PPh₃); ¹³C{¹H} NMR (101 MHz, THF-*d*₈): δ 213.7 (CO), 195.6 (C2-NHC), 150.2 (C_q arom), 138.7 (C_q arom), 137.3 (C_q arom), 137.2 (C_q arom), 137.0 (C_q arom), 135.0 (C_q arom), 128.7 (2 CH arom), 120.4 (2 CH arom), 119.3 (C^b), 117.6 (C^e), 116.7 (C^c), 95.9 (C^d), 59.6 (C(CH₃)₃), 57.6 (C^a), 35.9 (C(CH₃)₃), 21.1 (CH₃), 20.5 (CH₃), 18.4 ppm (CH₃).

Complex 8: In a J.Young valved NMR tube, THF-*d*₈ (0.5 mL) was added to a mixture of **3a** (0.022 g, 0.026 mmol) and KO^tBu (0.0038 g, 0.034 mmol) forming a dark red solution. Heating the resulting mixture to 60 °C for 24 h produced a dark blue solution that was analyzed by NMR spectroscopy. Attempted isolation of **8** was unsuccessful due to decomposition of the complex during work-up.



^1H NMR (400 MHz, THF- d_8): δ 7.92 (d, $^4J(\text{H},\text{P}) = 3.7$ Hz, 1H; $\text{CH}=\text{N}^t\text{Bu}$), 7.30 (d, $^3J(\text{H},\text{H}) = 2.0$ Hz, 1H; H arom, NHC), 7.12 (d, $^3J(\text{H},\text{H}) = 8.5$ Hz, 1H; H^d), 7.07 (m, 3H; 3 H arom, PPh_3), 7.00 (m, 7H; 6 H arom, PPh_3 + H arom, NHC), 6.91 (s, 1H; H arom, mes), 6.75 (m, 7H; 6 H arom PPh_3 + H arom, mes), 6.37 (ddd, $^3J(\text{H},\text{H}) = 8.5$ Hz, $^3J(\text{H},\text{H}) = 6.4$ Hz, $^6J(\text{H},\text{P}) = 4.3$ Hz, 1H; H^c), 5.79 (dd, $^3J(\text{H},\text{H}) = 6.4$ Hz, $^5J(\text{H},\text{P}) = 3.1$ Hz, 1H; H^b), 4.74 (d, $^2J(\text{H},\text{H}) = 14.0$ Hz, 1H; CHH-NHC), 3.91 (d, $^2J(\text{H},\text{H}) = 13.9$ Hz, 1H; CHH-NHC), 2.28 (s, 6H, 2 CH_3), 1.30 (s, 3H, CH_3), 1.23 ppm (s, 9H, $\text{C}(\text{CH}_3)_3$); $^{31}\text{P}\{^1\text{H}\}$ NMR (162 MHz, THF- d_8): δ 50.5 ppm; $^{13}\text{C}\{^1\text{H}\}$ NMR (101 MHz, THF- d_8): δ 216.1 (d, $J(\text{C},\text{P}) = 10$ Hz; CO), 191.3 (d, $J(\text{C},\text{P}) = 7$ Hz; C-2 NHC), 148.1 (C_q arom), 143.1 (C_q arom), 139.8 (d, $J(\text{C},\text{P}) = 34$ Hz; 3 C_q arom), 138.6 (C_q arom), 138.3 (C_q arom), 137.0 (C_q arom), 136.7 (C_q arom), 132.9 (d, $J_{\text{CP}} = 11$ Hz; 6 CH arom), 131.8 (d, $J(\text{C},\text{P}) = 3$ Hz; $\text{CH}=\text{N}^t\text{Bu}$), 129.4 (CH arom), 129.3 (CH arom), 128.1 (3 CH arom, PPh_3), 127.8 (d, $J(\text{C},\text{P}) = 9$ Hz; 6 CH arom), 123.5 (CH arom), 122.8 (d, $J(\text{C},\text{P}) = 5$ Hz; C^d), 121.6 (CH arom), 119.6 (d, $J(\text{C},\text{P}) = 4$ Hz; C^c), 107.5 (C^b), 63.1 (d, $J(\text{C},\text{P}) = 4$ Hz; $\text{C}(\text{CH}_3)_3$), 56.4 ($\text{CH}_2\text{-NHC}$), 33.9 (d, $J(\text{C},\text{P}) = 3$ Hz; $\text{C}(\text{CH}_3)_3$), 21.0 (CH_3), 20.3 (CH_3), 19.0 ppm (CH_3).

1.6. Catalytic reactions

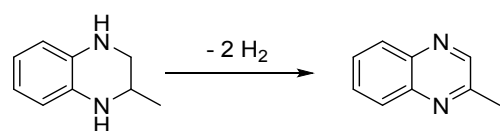
Representative procedure for catalytic hydrogenation reactions of N-heterocycles

In a glovebox, a Fischer–Porter vessel was charged with a solution of complex **3a** (1.0 mg, 1.2 μmol), KO^tBu (1.3 mg, 12 μmol) and quinoxaline (0.031 g, 0.24 mmol) in 2-methyltetrahydrofuran (1.0 mL). The reactor was purged three times with H_2 , and finally pressurized to 4 bar and heated to 80 $^\circ\text{C}$. After 6 h, the reactor was slowly cooled down to room temperature and depressurized. The reaction solution was evaporated, and conversion was determined by ^1H NMR spectroscopy using mesitylene as internal standard.

Representative procedure for catalytic dehydrogenation reactions of N-heterocycles

In a glovebox, a Schlenk tube was charged with a solution of complex **3a** (4.0 mg, 4.7 μmol), KO^tBu (8.0 mg, 71 μmol) and 1,2,3,4-tetrahydro-2-methylquinoxaline (**5b**) (17.7 mg, 119 μmol) in *o*-xylene (1.0 mL). A reflux condenser was adapted to the Schlenk flask, and the solution was heated to 160 $^\circ\text{C}$ under N_2 . After 24 h, the reaction solution was evaporated, and the residue was filtered through a short pad of silica (eluent: pentane \rightarrow Et_2O). Conversion was determined by ^1H NMR spectroscopy using mesitylene as internal standard.

To determine the influence of different of the base, a series of bases were tested in the dehydrogenation reaction of 1,2,3,4-tetrahydro-2-methylquinoxaline (Figure S1).



160 °C, *o*-xylene, 4.0 mol% **3a**, 60 mol% **base**, 24 h

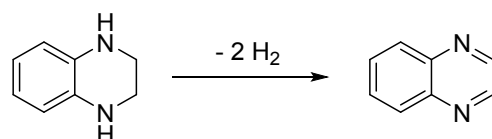
base = KO^tBu, 85% conv.

KHMDS, 84% conv.

NaH, 6% conv.

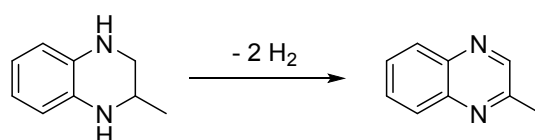
Figure S1. Influence of the base in the dehydrogenation of 1,2,3,4-tetrahydro-2-methylquinoxaline.

Furthermore, since KO^tBu has been shown to promote N-heterocycle dehydrogenation (typical conditions: 3 equiv. KO^tBu, *o*-xylene, 140 °C),³ control experiments were performed with selected substrates in the absence of the Ru catalyst (Figure S2).



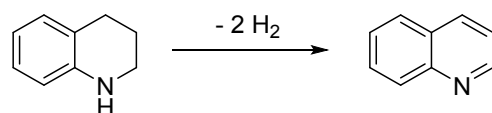
85 °C, 2-MeTHF, 4.0 mol% **3a**, 60 mol% KO^tBu, 24 h
(Table 2, entry 1): > 99% NMR yield

85 °C, 2-MeTHF, 60 mol% KO^tBu, 24 h: 0% NMR yield



160 °C, *o*-xylene, 4.0 mol% **3a**, 60 mol% KO^tBu, 24 h
(Table 2, entry 2): 85% NMR yield

160 °C, *o*-xylene, 60 mol% KO^tBu, 24 h: < 5% NMR yield



160 °C, *o*-xylene, 4.0 mol% **3a**, 60 mol% KO^tBu, 48 h
(Table 2, entry 6): 50% NMR yield

160 °C, *o*-xylene, 60 mol% KO^tBu, 48 h: 0% NMR yield

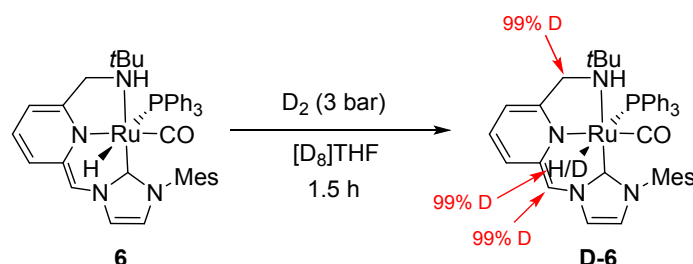
³ T. Liu, K. Wu, L. Wang and Z. Yu, *Adv. Synth. Catal.*, 2019, **361**, 3958

Figure S2. Influence of KO^tBu and **3a** in the dehydrogenation of N-heterocycles.

2. Reactions of complexes **6**, **7** and **8** with D₂

Deuteration of complex **6** with D₂

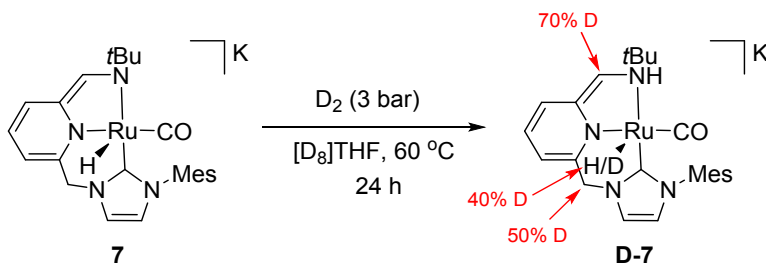
In a J. Young valved NMR tube, THF-*d*₈ (0.5 mL) was added to a mixture of **3a** (0.023 g, 0.027 mmol) and KO^tBu (0.004 g, 0.035 mmol), giving rise to the immediate formation of a dark red solution of complex **6**. The NMR tube was pressurized with 3 bar of D₂, and analyzed by ¹H NMR spectroscopy after 1.5 h.



Scheme S1. H/D scrambling in complex **6**, generated from **3a** and KO^tBu (1.3 equiv), upon exposure to D₂ in THF-*d*₈.

Deuteration of complex **7** with D₂

In a J. Young valved NMR tube, THF-*d*₈ (0.5 mL) was added to a mixture of **3a** (0.025 g, 0.030 mmol) and KHMDS (0.018 g, 0.090 mmol) giving rise initially to a dark red solution that gradually evolved to dark violet. After 24 h, the NMR tube was pressurized with 3 bar of D₂, heated to 60 °C for 24 h and analyzed by ¹H NMR spectroscopy.



Scheme S2. H/D scrambling in complex **7**, generated from **3a** and KHMDS (3.0 equiv), upon exposure to D₂ in THF-*d*₈.

Reaction of complex **8** with D₂

In a J.Young valved NMR tube, a mixture of **3a** (0.018 g, 0.021 mmol) and KO^tBu (0.003 g, 0.028 mmol) in THF-*d*₈ (0.5 mL) was heated to 60 °C overnight, yielding complex **8** and ^tBuOH (Figure S3, a). The sample was pressurized with D₂ (3 bar) and heated to 65 °C for 24 h (Figure S3, b). Formation of HD and H₂ was observed by ¹H NMR spectroscopy (H₂: δ 4.54 ppm; HD: δ 4.51 ppm, *J*_{HD} = 42.7 Hz) (Figure S3, c).

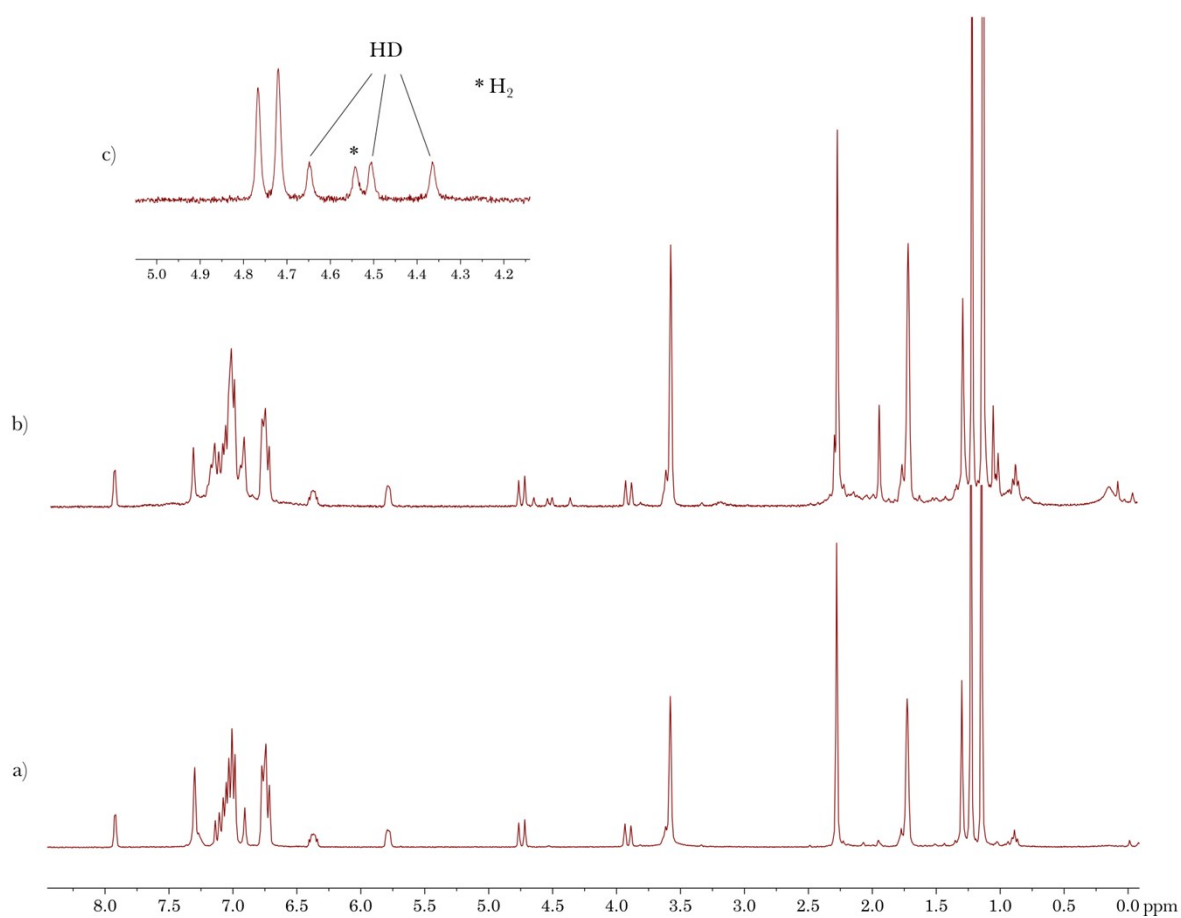


Figure S3. ¹H NMR spectra (300 MHz) of: a) a heated solution (60 °C) of the reaction of **3a** with KO^tBu in THF-*d*₈ to yield **8**; and b) pressurization with 3 bar of D₂ of the same reaction [c) corresponds to the enlarged 4.2-5.0 ppm region of the spectrum b)].

3. NMR spectroscopy monitoring of hydrogenation reactions

Experiment 1

In a J.Young valved NMR tube, a mixture of **3a** (0.007 g, 0.008 mmol) and KHMDS (0.003 g, 0.017 mmol) in THF-*d*₈ (0.5 mL) was heated overnight to 60 °C to yield complex **8**. 2-Methylquinoxaline (0.012 g, 0.080 mmol) was added, and the sample was pressurized with H₂ (3 bar) (Figures S4a and S5a). The sample was heated to 60 °C in the NMR spectrometer, and reaction progress was monitored by ¹H and ³¹P{¹H} NMR spectroscopy (Figures S4b-S4d and S5b-S5d).

In an analogous experiment using KO^tBu as base, significant line broadening was observed in the ¹H NMR spectra after addition of 2-methylquinoxaline precluding reaction follow-up. However, monitoring of the catalytic reaction by ³¹P{¹H} NMR spectra only showed a resonance at 53.0 ppm (s) due to complex **8**.

Experiment 2

In a J.Young valved NMR tube, a mixture of **3a** (0.015 g, 0.018 mmol) and KHMDS (0.013 g, 0.064 mmol) was dissolved in THF-*d*₈ (0.7 mL). The mixture was analyzed by NMR spectroscopy after 1 h, showing the formation of complexes **6** and **7** (1:1 ratio) (Figures S6a and S7a). 2-Methylquinoxaline (0.026 g, 0.178 mmol) was added to the sample, and analysis by NMR indicated the immediate formation of complex **8** (significant signal broadening of the substrate resonances were observed in the spectra) (Figures S6b and S7b). The sample was pressurized with H₂ (3 bar) (Figures S6c and S7c), and heated to 65 °C for 1 h producing the formation of 1,2,3,4-tetrahydro-2-methylquinoxaline (aprox. 80% conv) (Figures S6d and S7d).

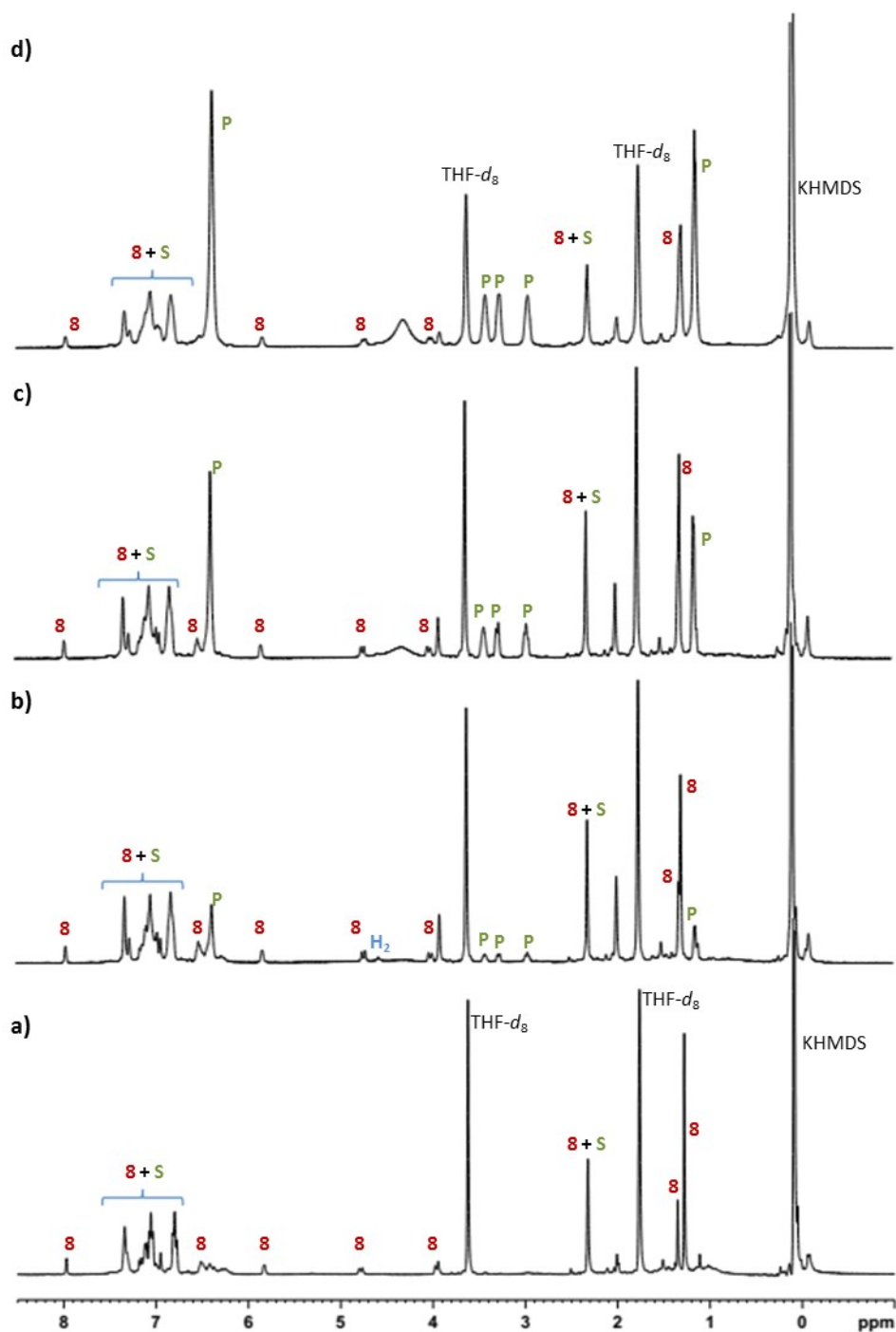


Figure S4. ^1H NMR spectra (400 MHz, 60 $^\circ\text{C}$) of a) complex **8** (formed in situ from **3a** and KHMDS), 2-methylquinoxaline (10 equiv) and H_2 (4 bar); b) after heating to 60 $^\circ\text{C}$ for 5 min; c) after heating to 60 $^\circ\text{C}$ for 10 min; d) after heating to 60 $^\circ\text{C}$ for 20 min (**S**: 2-methylquinoxaline; **P**: 1,2,3,4-tetrahydro-2-methylquinoxaline). (no signals were observed in the hydride region of the ^1H NMR spectra)

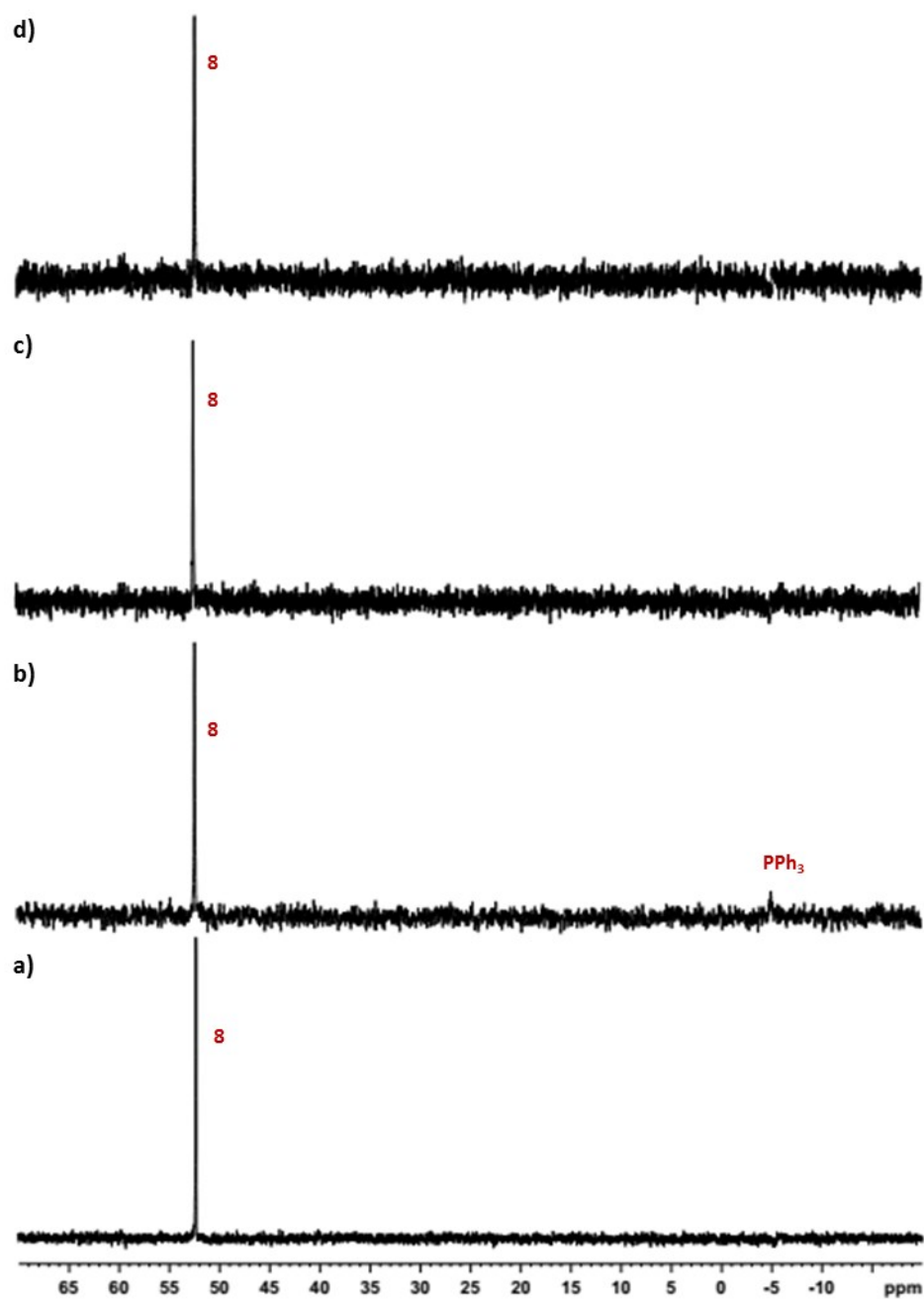


Figure S5. $^{31}\text{P}\{^1\text{H}\}$ NMR spectra (162 MHz, 60 °C) of a) complex **8** (formed in situ from **3a** and KHMDS), 2-methylquinoxaline (10 equiv) and H_2 (4 bar); b) after heating to 60 °C for 5 min; c) after heating to 60 °C for 10 min; d) after heating to 60 °C for 20 min (**S**: 2-methylquinoxaline; **P**: 1,2,3,4-tetrahydro-2-methylquinoxaline).

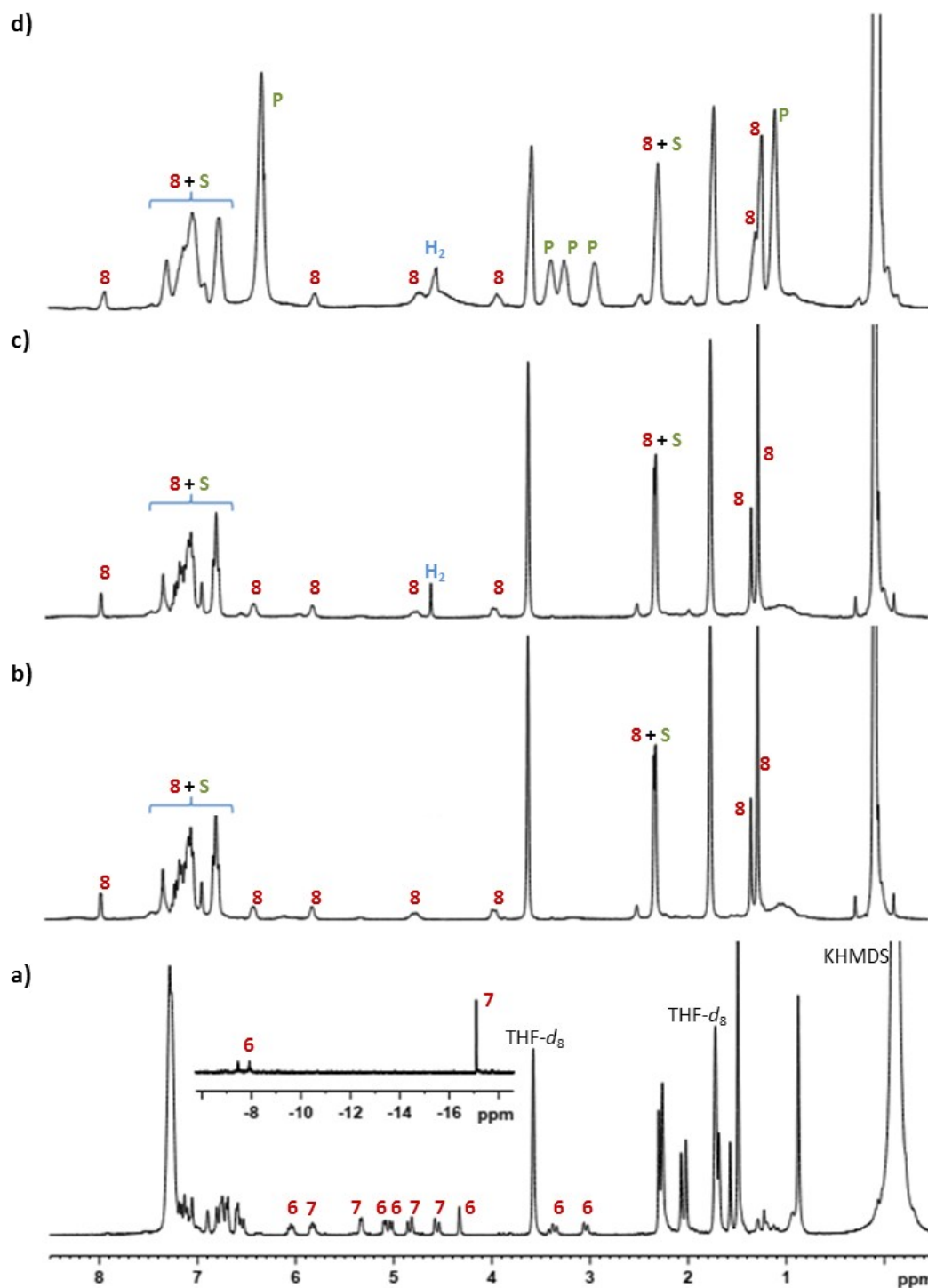


Figure S6. ¹H NMR spectra (300 MHz, 25 °C) of a) the reaction of **3a** with KHMDS to yield **6** and **7**; b) after addition of 2-methylquinoxaline; c) pressurization with 3 bar of H₂; and d) heating at 65 °C for 1 h (**S**: 2-methylquinoxaline; **P**: 1,2,3,4-tetrahydro-2-methylquinoxaline).

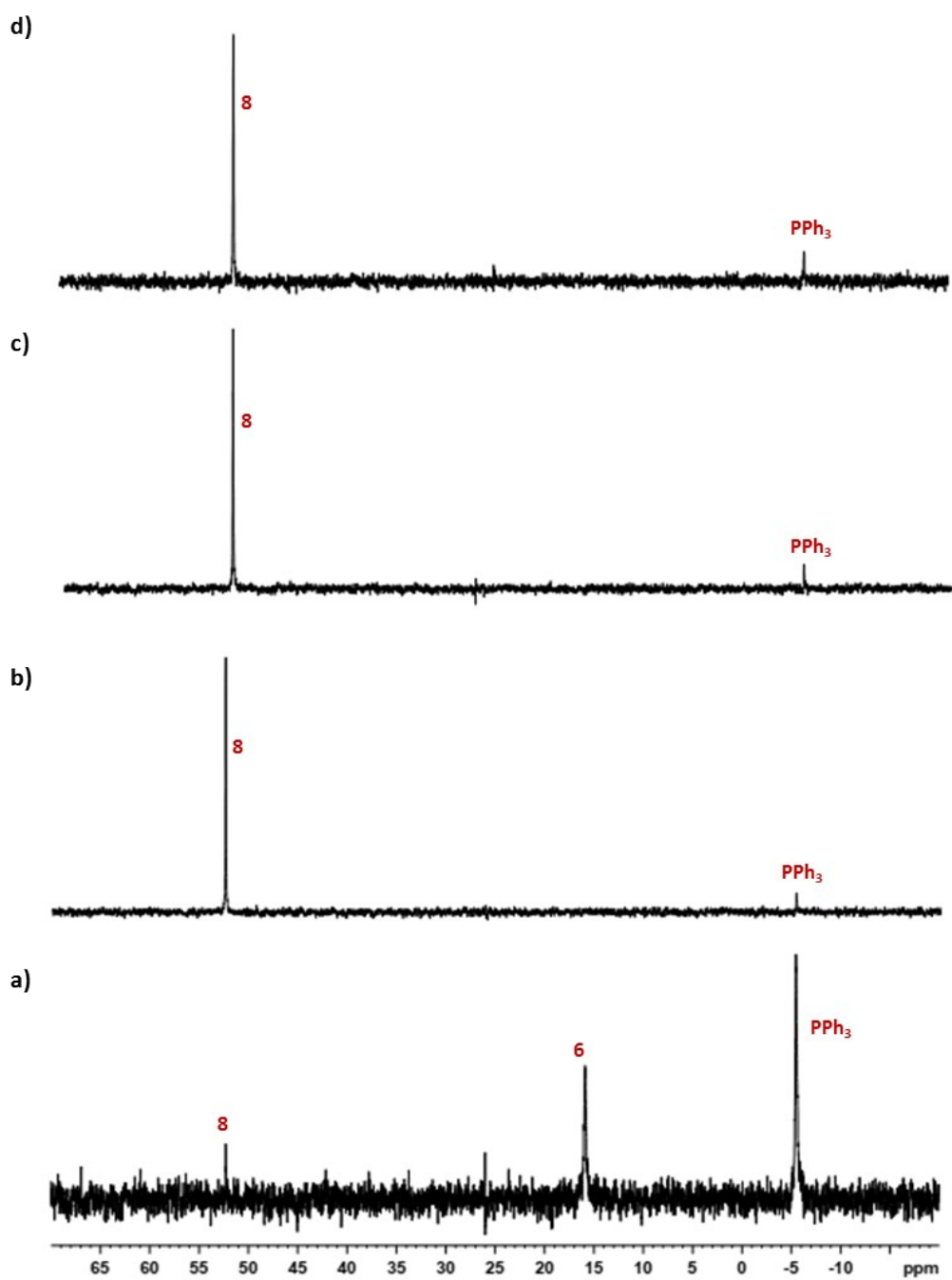


Figure S7. $^{31}\text{P}\{^1\text{H}\}$ NMR spectra (121 MHz, 25 °C) of a) the reaction of **3a** with KHMDS to yield **6** and **7**; b) after addition of 2-methylquinoxaline; c) pressurization with 3 bar of H_2 ; and d) heating to 65 °C for 1 h (**S**: 2-methylquinoxaline; **P**: 1,2,3,4-tetrahydro-2-methylquinoxaline).

4. X-Ray structure analysis of complexes **3a** and **3b**

Crystals suitable for X-ray diffraction analysis were coated with dry perfluoropolyether, mounted on glass fibers, and fixed in a cold nitrogen stream to the goniometer head. Data collections were performed on a Bruker-Nonius X8 Apex-II CCD diffractometer, using graphite monochromatized Mo radiation ($\lambda(\text{Mo } K\alpha) = 0.71073 \text{ \AA}$) and fine-sliced ω and φ scans (scan widths 0.30° to 0.50°).⁴ The data were reduced (*SAINTE*) and corrected for absorption effects by the multiscan method (*SADABS*).⁵ The structures were solved by direct methods (*SIR2002*, *SHELXS*) and refined against all F^2 data by full-matrix least-squares techniques (*SHELXL-2016/6*) minimizing $w[F_o^2 - F_c^2]^2$.⁶ All non-hydrogen atoms were refined with anisotropic displacement parameters. Hydrogen atoms were included in calculated positions and allowed to ride on their carrier atoms with the isotropic temperature factors U_{iso} fixed at 1.2 times (1.5 times for methyl groups) of the U_{eq} values of the respective carrier atoms. The asymmetric unit of **3a** presents one salt of the ruthenium complex and one dichloromethane molecule of crystallization that appears disordered, so this solvent molecule was modeled in two sets of sites. At the end of the refinement the occupancy coefficients were set at 0.5 for both. Moreover, a search for solvent accessible voids for the crystal structure of **3a** using *PLATON*,⁷ showed some small volumes of potential solvents less than 251 \AA^3 (95 electron count), impossible to model even with the most severe restraints. The corresponding CIF data represent *SQUEEZE*⁸ treated structures with the solvent molecules handling as a diffuse contribution to the overall scattering, without specific atom position and excluded from the structural model. The *SQUEEZE* results were appended to the CIF. The asymmetric unit of **3b** presents one complex salt of the ruthenium where the anion BF_4 appears disordered and was modeled in two sets of sites. At the end of the refinement the occupancy coefficients were set at 0.67 and 0.33, respectively. Next to this ruthenium complex there are two methanol molecules of crystallization that not present disorder. The modeling of the observed disorders described above required some geometric restraints (DFIX instruction), the ADP restraint SIMU and the rigid bond restraint DELU were used in order to obtain more reasonable geometric and

⁴ Bruker *APEX2*; Bruker AXS, Inc.; Madison, WI, 2007.

⁵ Bruker Advanced X-ray solutions. *SAINTE* and *SADABS* programs. Bruker AXS Inc. Madison, WI, 2004.

⁶ M. C. Burla, M. Camalli, B. Carrozzini, G. L. Casciarano, C. Giacovazzo, G. Polidori, R. Spagna. *SIR2002: the Program*. *J. Appl. Crystallogr.* 2003, **36**, 1103–1104.

⁷ A. L. Spek. Single-crystal Structure Validation with the Program *PLATON*. *J. Appl. Crystallogr.* 2003, **36**, 7-13.

⁸ P. v. d. Sluis, A. L. Spek. *BYPASS: An Effective Method for the Refinement of Crystal Structures Containing Disordered Solvent Regions*. *Acta Crystallogr., Sect. A*. 1990, **46**, 194-201.

ADP values of the disordered atoms. It was also useful to restrain the anisotropic U-values of these atoms to behave more isotropically (ISOR instruction). A summary of cell parameters, data collection, structures solution, and the refinement of crystal structures are provided below. The corresponding crystallographic data were deposited with the Cambridge Crystallographic Data Centre as supplementary publications. CCDC 1968868 (**3a**) and 1968869 (**3b**). The data can be obtained free of charge via: <https://www.ccdc.cam.ac.uk/structures/>

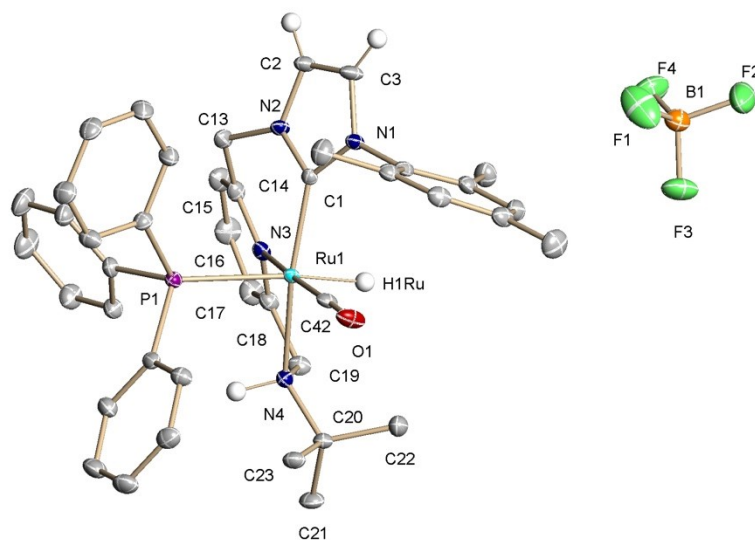


Figure S8. ORTEP view of molecular structure of the ruthenium salt complex **3a** with thermal ellipsoids drawn at the 30% level. Hydrogen atoms, except the hydride ligand, the amine hydrogen and the NHC hydrogens, have been omitted for clarity.

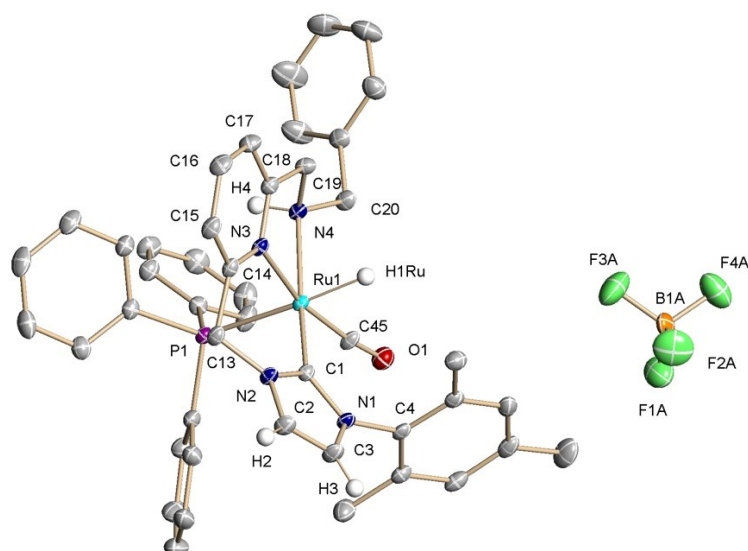


Figure S9. ORTEP view of molecular structure of the ruthenium salt complex **3b** with thermal ellipsoids drawn at the 30% level. Hydrogen atoms, except the hydride ligand, the amine hydrogen and the NHC hydrogens, have been omitted for clarity.

Table S1. Crystal data and structure refinement for **3a**

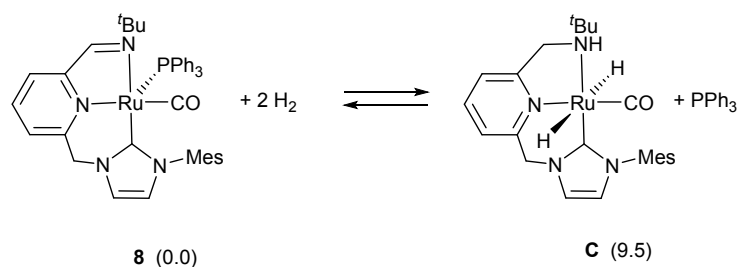
Empirical formula	C ₄₃ H ₄₈ BCl ₂ F ₄ N ₄ OPRu [C ₄₂ H ₄₆ N ₄ OPRu, BF ₄ , CH ₂ Cl ₂]	
Formula weight	926.60	
Temperature	193(2) K	
Wavelength	0.71073 Å	
Crystal system	Triclinic	
Space group	p $\bar{1}$	
Unit cell dimensions	a = 11.3501(2) Å	α = 101.8900(10)°.
	b = 13.8331(3) Å	β = 99.4460(10)°.
	c = 15.6821(4) Å	γ = 95.6230(10)°.
Volume	2354.45(9) Å ³	
Z	2	
Density (calculated)	1.307 Mg/m ³	
Absorption coefficient	0.531 mm ⁻¹	
F(000)	952	
Crystal size	0.450 x 0.400 x 0.350 mm ³	
Theta range for data collection	1.790 to 25.250°.	
Index ranges	-13 ≤ h ≤ 13, -16 ≤ k ≤ 16, -18 ≤ l ≤ 18	
Reflections collected	33376	
Independent reflections	8542 [R(int) = 0.0152]	
Completeness to theta = 25.242°	99.9 %	
Absorption correction	Semi-empirical from equivalents	
Max. and min. transmission	0.7461 and 0.6886	
Refinement method	Full-matrix least-squares on F ²	
Data / restraints / parameters	8542 / 85 / 547	
Goodness-of-fit on F ²	1.089	
Final R indices [I > 2σ(I)]	R1 = 0.0323, wR2 = 0.1319	
R indices (all data)	R1 = 0.0338, wR2 = 0.1358	
Extinction coefficient	n/a	
Largest diff. peak and hole	0.934 and -0.677 e.Å ⁻³	

Table S2. Crystal data and structure refinement for **3b**

Empirical formula	$C_{47}H_{52}BF_4N_4O_3PRu$ [$C_{45}H_{44}N_4OPRu$, BF_4 , $2(CH_4O)$]
Formula weight	939.77
Temperature	193(2) K
Wavelength	0.71073 Å
Crystal system	Triclinic
Space group	$P\bar{1}$
Unit cell dimensions	$a = 11.4403(2)$ Å $\alpha = 70.0200(10)^\circ$ $b = 14.1416(2)$ Å $\beta = 80.3220(10)^\circ$ $c = 15.3495(2)$ Å $\gamma = 89.7150(10)^\circ$
Volume	$2296.93(6)$ Å ³
Z	2
Density (calculated)	1.359 Mg/m ³
Absorption coefficient	0.436 mm ⁻¹
F(000)	972
Crystal size	0.500 x 0.400 x 0.300 mm ³
Theta range for data collection	2.305 to 25.250°.
Index ranges	-13 ≤ h ≤ 13, -16 ≤ k ≤ 16, -14 ≤ l ≤ 18
Reflections collected	38516
Independent reflections	8314 [R(int) = 0.0152]
Completeness to theta = 25.242°	99.9 %
Absorption correction	Semi-empirical from equivalents
Max. and min. transmission	0.7461 and 0.7069
Refinement method	Full-matrix least-squares on F ²
Data / restraints / parameters	8314 / 171 / 605
Goodness-of-fit on F ²	1.054
Final R indices [I > 2σ(I)]	R1 = 0.0357, wR2 = 0.0943
R indices (all data)	R1 = 0.0377, wR2 = 0.0958
Extinction coefficient	n/a
Largest diff. peak and hole	1.426 and -0.779 e.Å ⁻³

5. DFT calculations

DFT calculations were carried out with the Gaussian 09 program.⁹ The hybrid functional B3LYP¹⁰ was used, with dispersion effects taken into account by adding the D3 version of Grimme's empirical dispersion.¹¹ C, H, N, O and P atoms were represented by the 6-31g(d,p) basis set,¹² whereas Ru was described using the Stuttgart/Dresden Effective Core Potential and its associated basis set SDD.¹³ All geometry optimizations were performed without restrictions in THF (bulk solvent effects modelled with the SMD continuum model).¹⁴



Scheme S3. Relative stabilities (ΔG in THF; kcal/mol) of complexes **8** and **C**.

⁹ M. J. Frisch, G. W. Trucks, H. B. Schlegel, G. E. Scuseria, M. A. Robb, J. R. Cheeseman, G. Scalmani, V. Barone, G. A. Petersson, H. Nakatsuji, X. Li, M. Caricato, A. Marenich, J. Bloino, B. G. Janesko, R. Gomperts, B. Mennucci, H. P. Hratchian, J. V. Ortiz, A. F. Izmaylov, J. L. Sonnenberg, D. Williams-Young, F. Ding, F. Lipparini, F. Egidi, J. Goings, B. Peng, A. Petrone, T. Henderson, D. Ranasinghe, V. G. Zakrzewski, J. Gao, N. Rega, G. Zheng, W. Liang, M. Hada, M. Ehara, K. Toyota, R. Fukuda, J. Hasegawa, M. Ishida, T. Nakajima, Y. Honda, O. Kitao, H. Nakai, T. Vreven, K. Throssell, J. A. Montgomery Jr., J. E. Peralta, F. Ogliaro, M. Bearpark, J. J. Heyd, E. Brothers, K. N. Kudin, V. N. Staroverov, T. Keith, R. Kobayashi, J. Normand, K. Raghavachari, A. Rendell, J. C. Burant, S. S. Iyengar, J. Tomasi, M. Cossi, J. M. Millam, M. Klene, C. Adamo, R. Cammi, J. W. Ochterski, R. L. Martin, K. Morokuma, O. Farkas, J. B. Foresman, D. J. Fox, Gaussian 09, Revision E.01, Gaussian, Inc., Wallingford CT, 2016.

¹⁰ a) A. D. Becke, *J. Chem. Phys.* 1993, **98**, 5648–5652; b) C. Lee, W. Yang, R. G. Parr, *Phys. Rev. B: Condens. Matter Mater. Phys.* 1988, **37**, 785–789; c) B. Miehlich, A. Savin, H. Stoll, H. Preuss, *Chem. Phys. Lett.* 1989, **157**, 200–206.

¹¹ S. Grimme, S. Ehrlich, L. Goerigk, *J. Comput. Chem.* 2011, **32**, 1456–1465.

¹² a) R. Ditchfield, W. J. Hehre, J. A. Pople, *J. Chem. Phys.* 1971, **54**, 724–728; b) W. J. Hehre, R. Ditchfield, J. A. Pople, *J. Chem. Phys.* 1972, **56**, 2257–2261; c) P. C. Hariharan, J. A. Pople, *Theor. Chim. Acta* 1973, **28**, 213–222; d) M. M. Francl, W. J. Pietro, W. J. Hehre, J. S. Binkley, M. S. Gordon, D. J. DeFrees, J. A. Pople, *J. Chem. Phys.* 1982, **77**, 3654–3665.

¹³ D. Andrae, U. Haeussermann, M. Dolg, H. Stoll, H. Preuss, *Theor. Chim. Acta* 1990, **77**, 123–141.

¹⁴ A. V. Marenich, C. J. Cramer, D. G. Truhlar, *J. Phys. Chem. B* 2009, **113**, 6378–6396.

6. Selected NMR spectra of complexes 2-8

6.1. Selected NMR spectra for complexes 2a-c

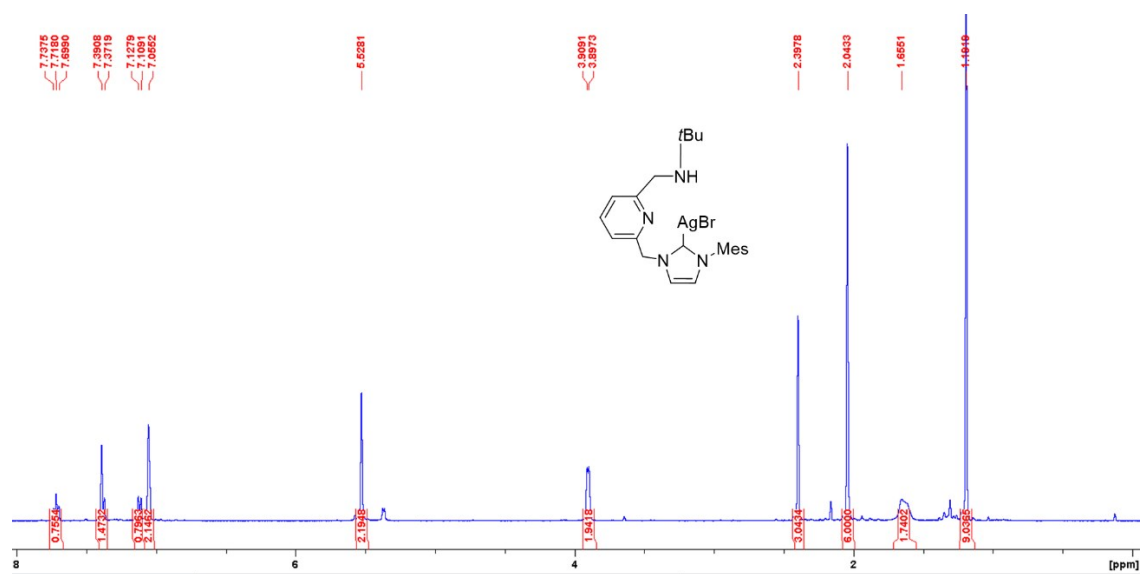


Figure S10. ^1H NMR spectrum (400 MHz) of **2a** in CD_2Cl_2 .

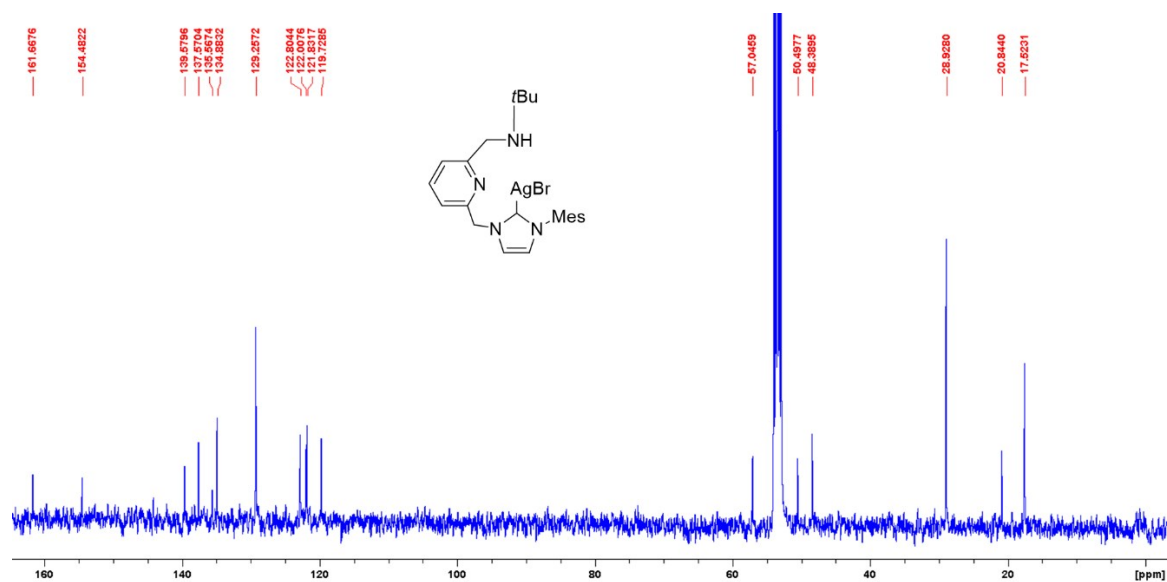


Figure S11. $^{13}\text{C}\{^1\text{H}\}$ NMR spectrum (101 MHz) of **2a** in CD_2Cl_2 .

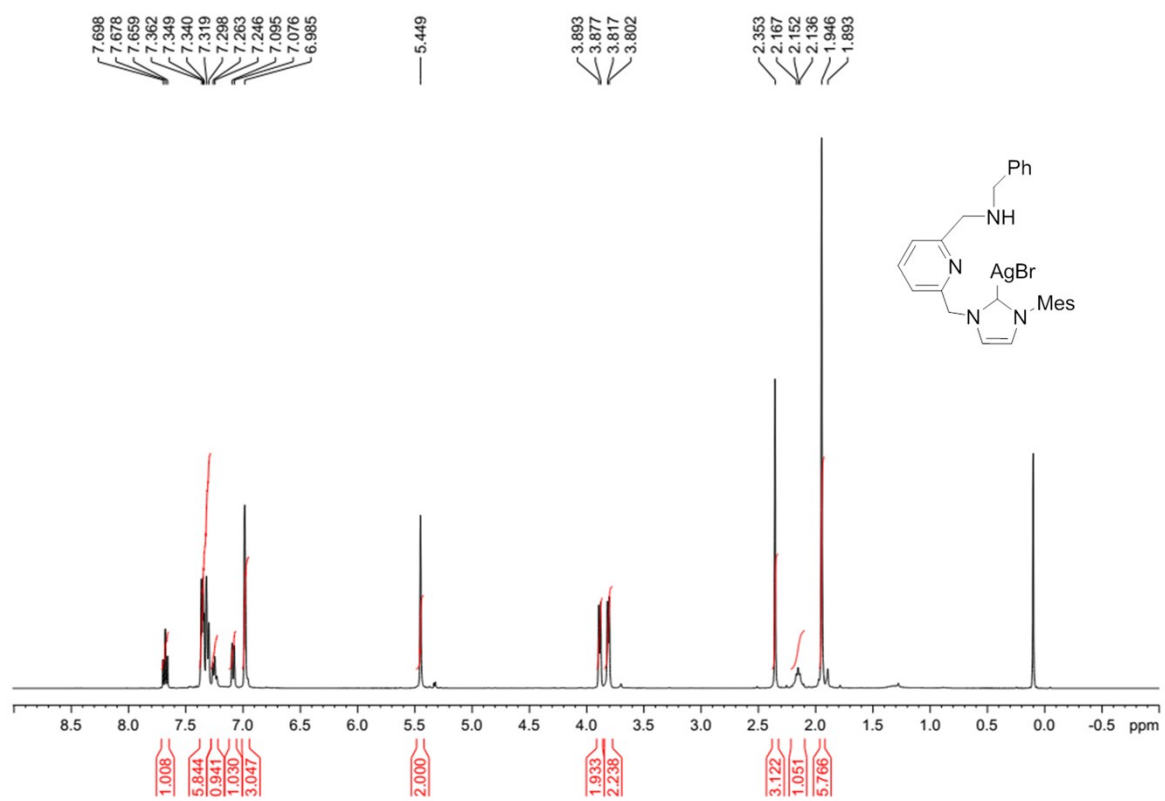


Figure S12. ¹H NMR spectrum (400 MHz) of **2b** in CD₂Cl₂.

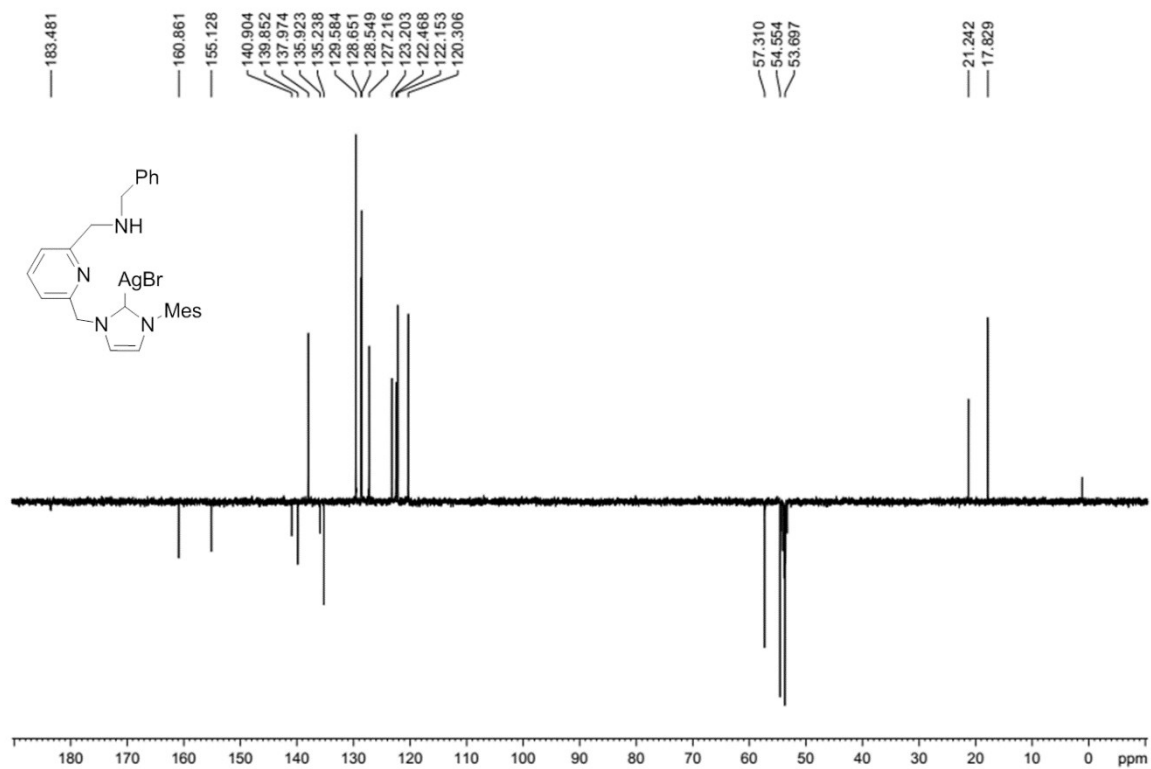


Figure S13. DEPT spectrum (101 MHz) of **2b** in CD₂Cl₂.

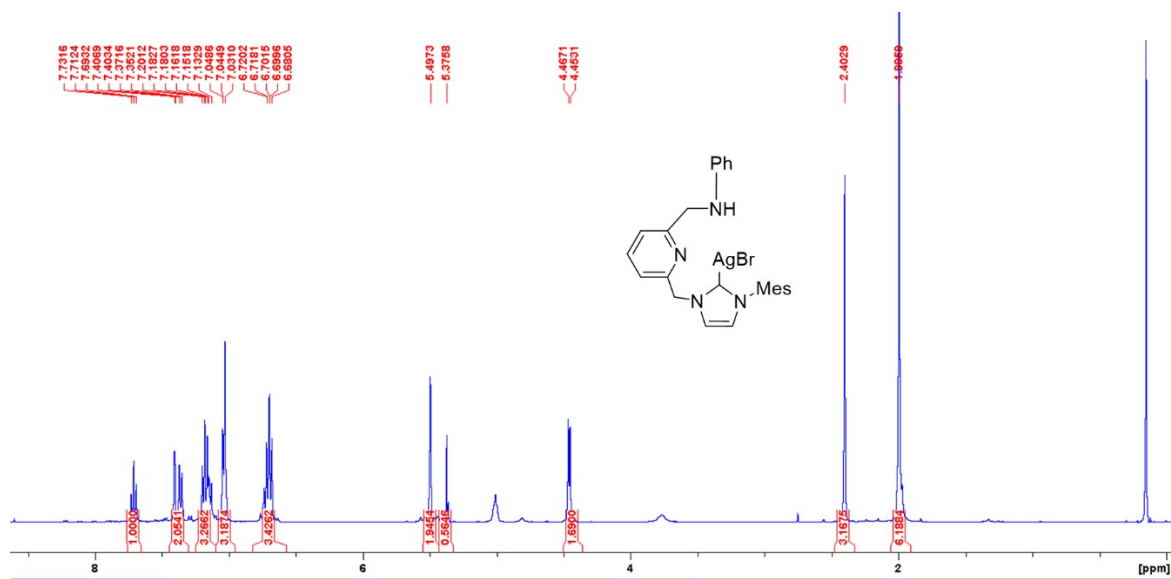


Figure S14. ¹H NMR spectrum (400 MHz) of **2c** in CD₂Cl₂.

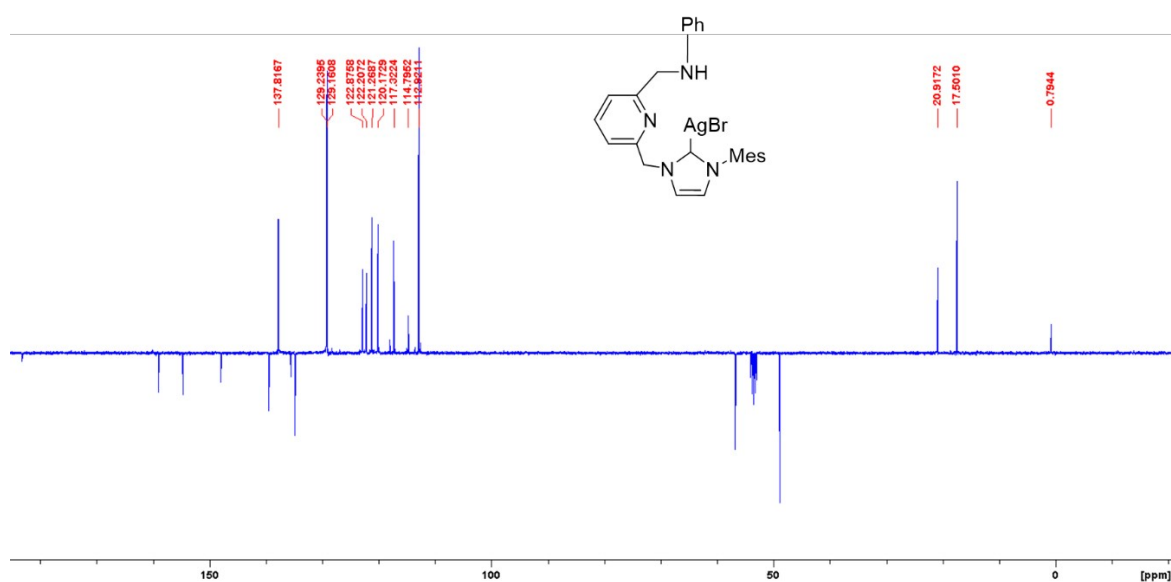


Figure S15. DEPT spectrum (101 MHz) of **2c** in CD₂Cl₂.

6.2. Selected NMR spectra for complexes 3a-c

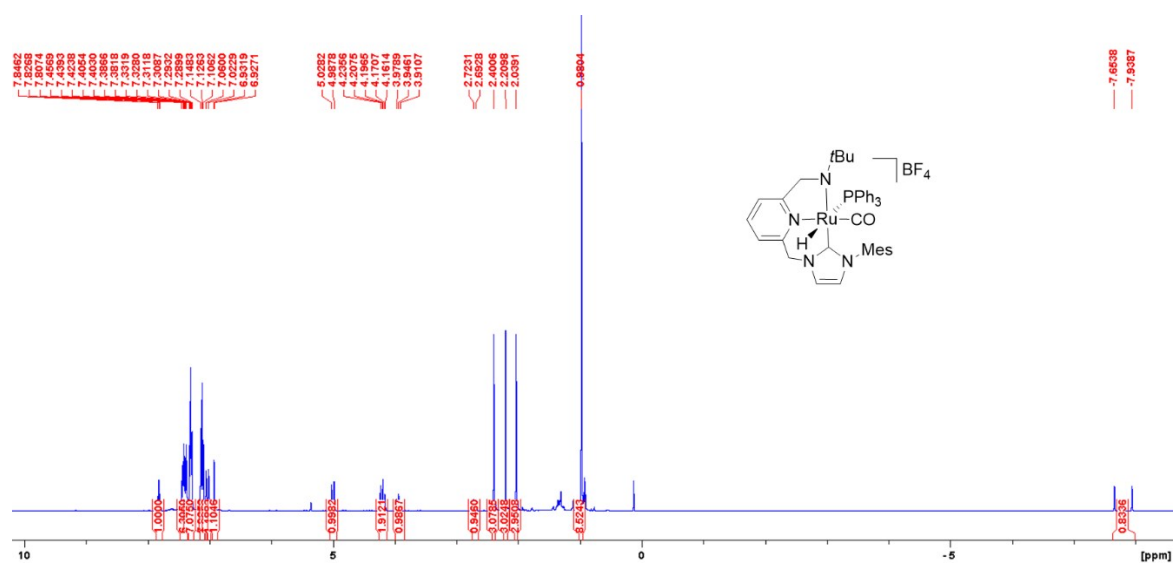


Figure S16. ¹H NMR spectrum (400 MHz) of 3a in CD₂Cl₂.

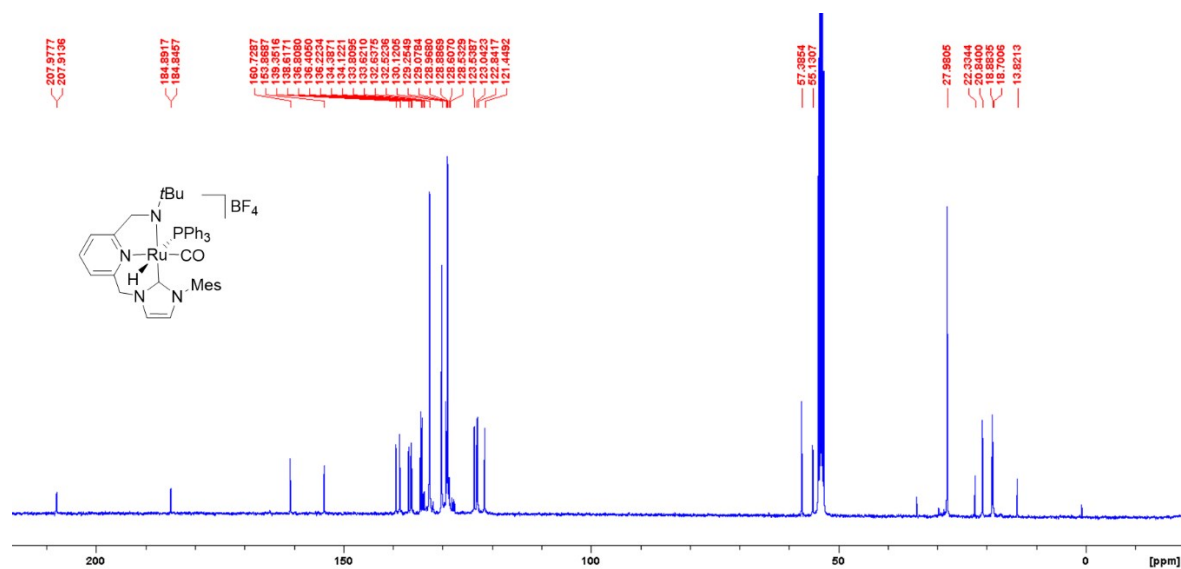


Figure S17. ¹³C{¹H} NMR spectrum (101 MHz) of 3a in CD₂Cl₂.

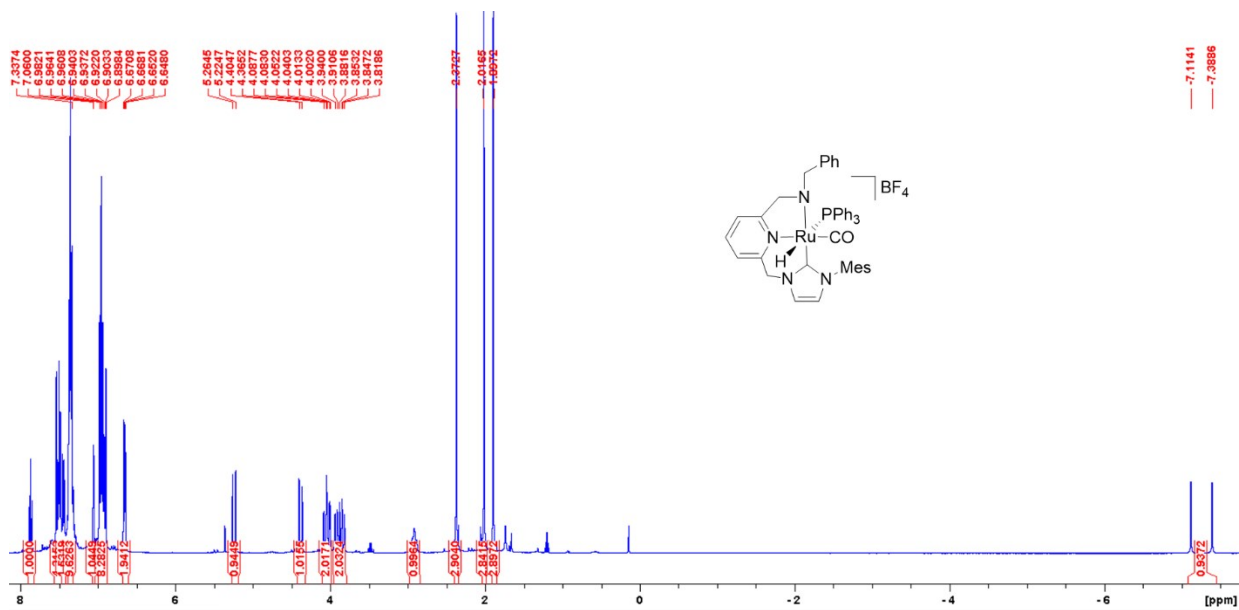


Figure S18. ¹H NMR spectrum (400 MHz) of **3b** in CD₂Cl₂.

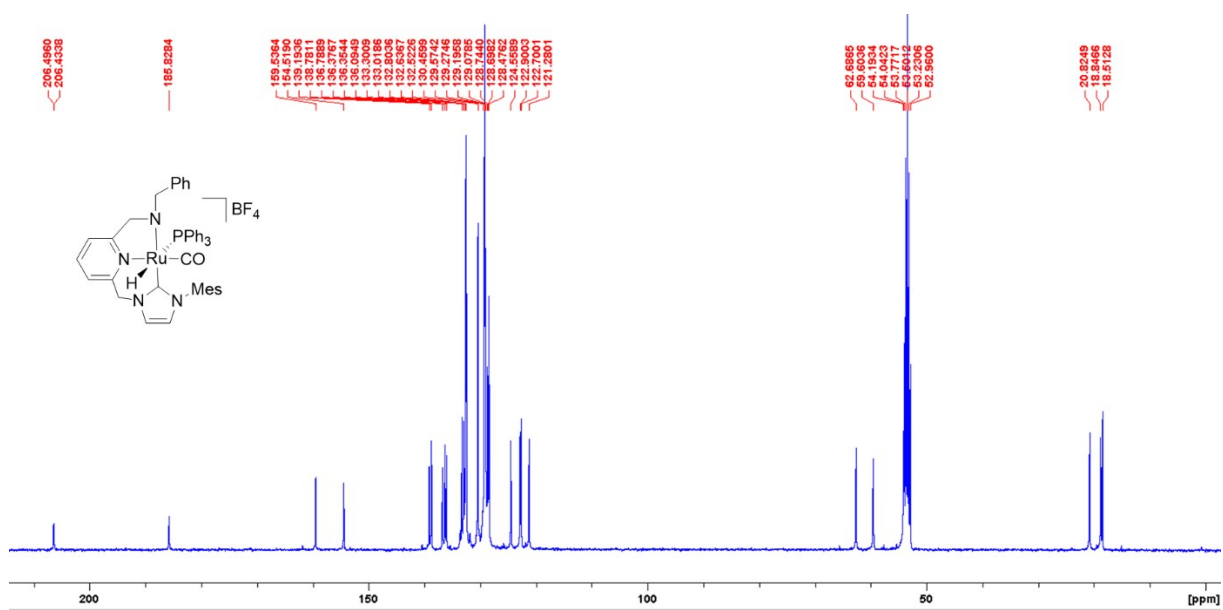


Figure S19. ¹³C{¹H} NMR spectrum (101 MHz) of **3b** in CD₂Cl₂.

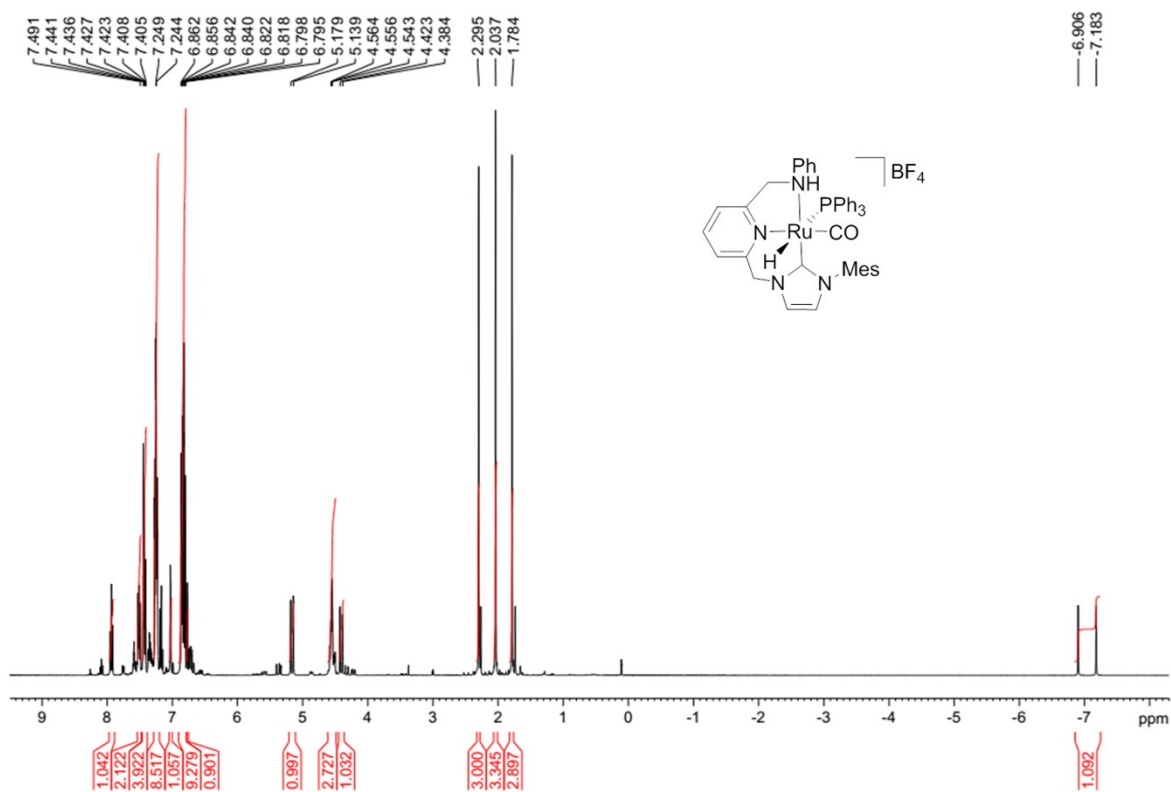


Figure S20. ¹H NMR spectrum (400 MHz) of **3c** in CD₂Cl₂.

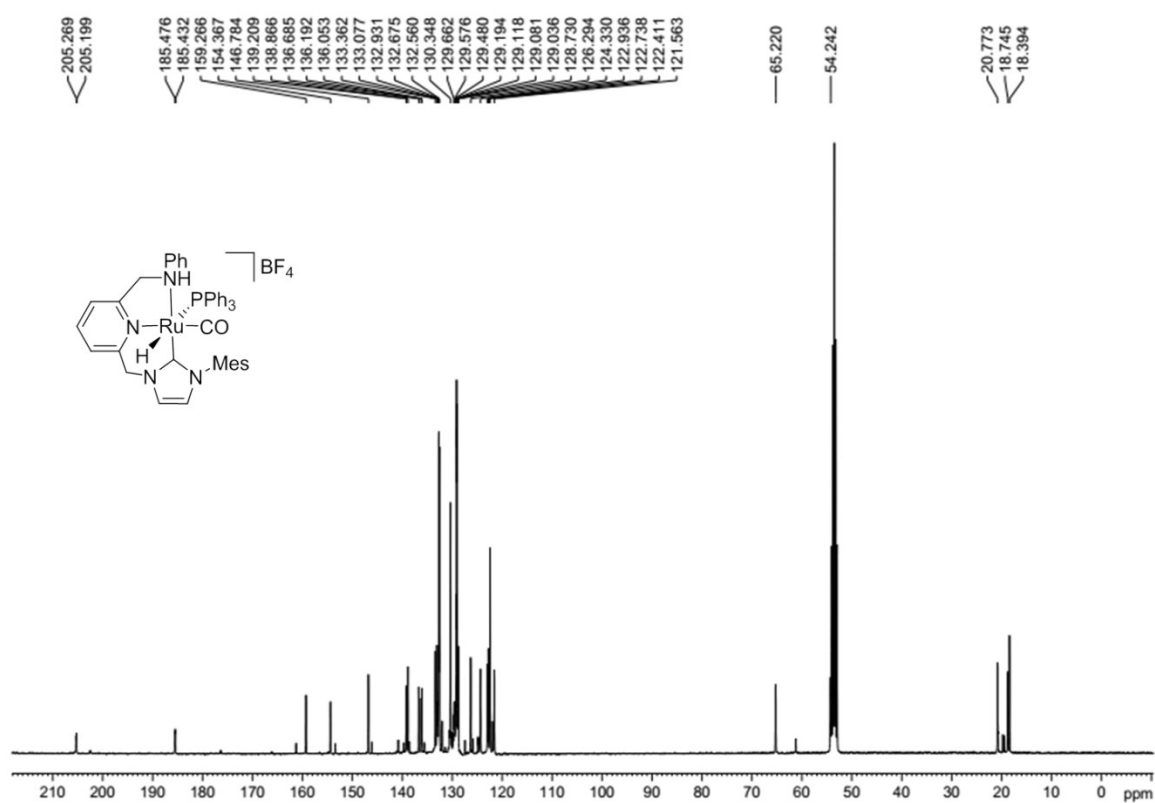


Figure S21. ¹³C{¹H} NMR spectrum (101 MHz) of **3c** in CD₂Cl₂.

6.3. Selected NMR spectra for complex 6

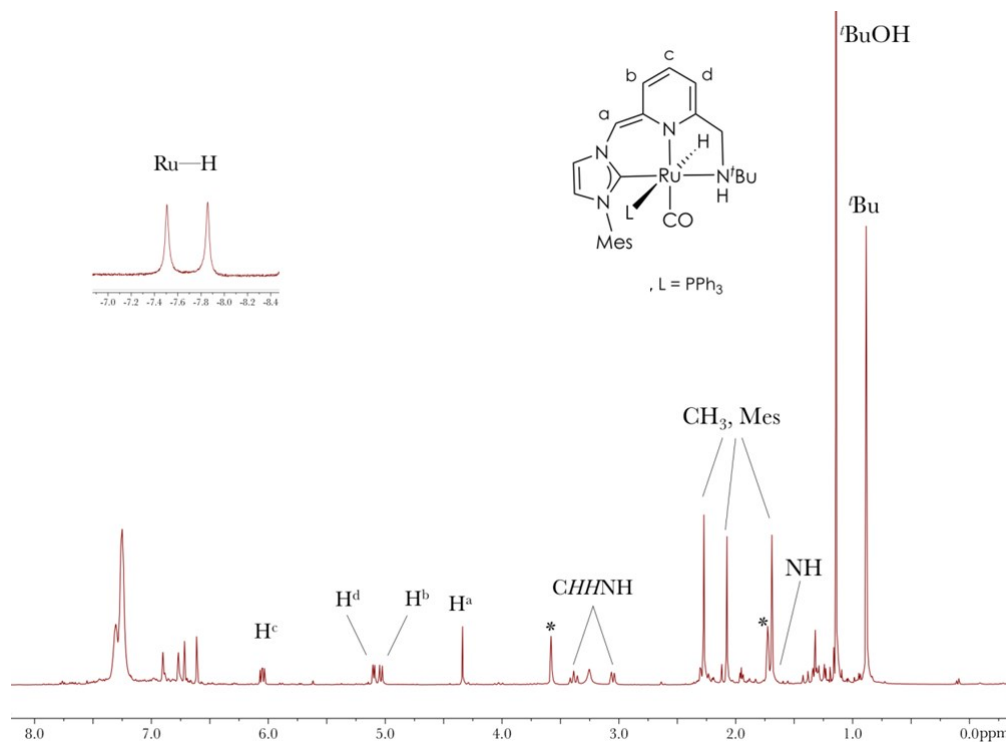


Figure S22. ^1H NMR spectrum (400 MHz) of the reaction of **3a** with KO^tBu in THF-*d*₈ to yield **6** (* denotes residual THF).

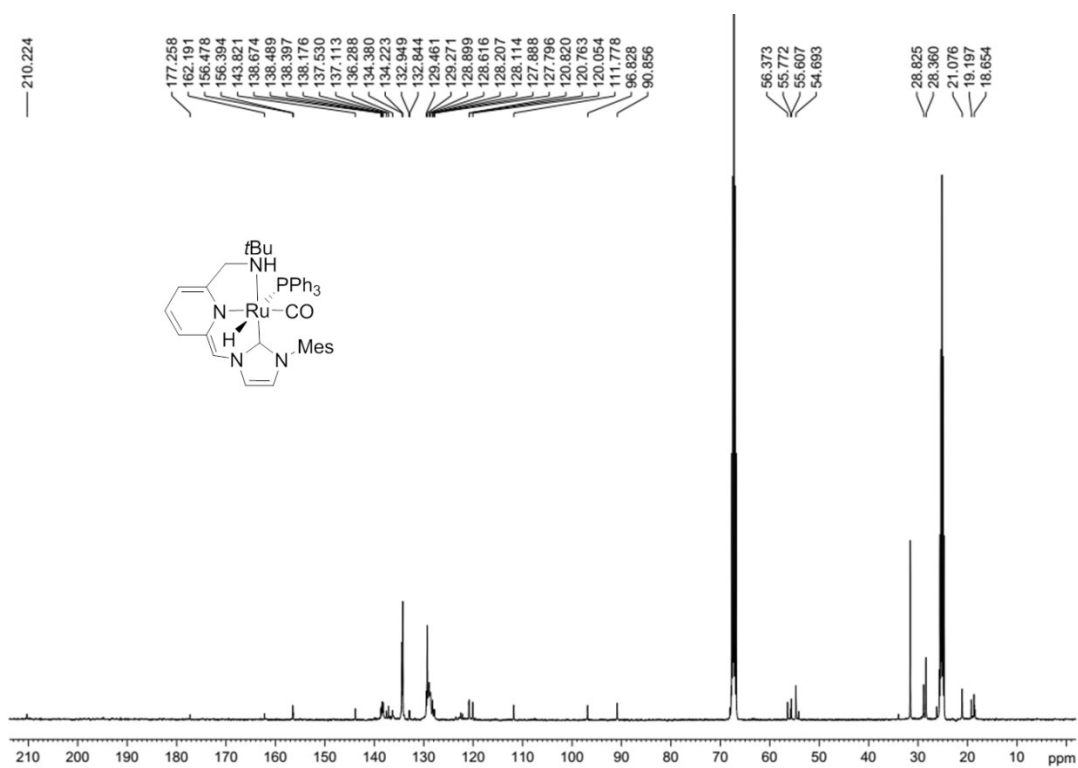


Figure S23. $^{13}\text{C}\{^1\text{H}\}$ NMR spectrum (101 MHz) of the reaction of **3a** with KO^tBu in THF-*d*₈ to yield **6**.

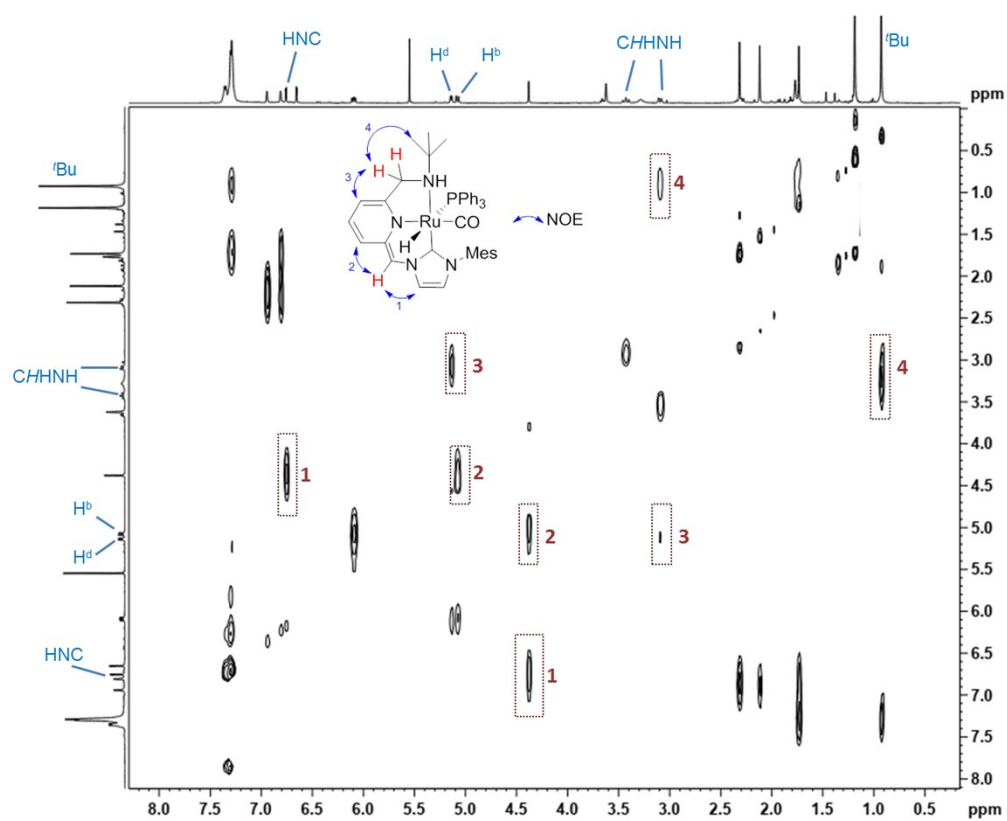


Figure S24. Selected region of the ^1H - ^1H NOESY spectrum (400 MHz) of the reaction of **3a** with KO^tBu in THF- d_6 to yield **6**.

6.4. Selected NMR spectra for complex **7**

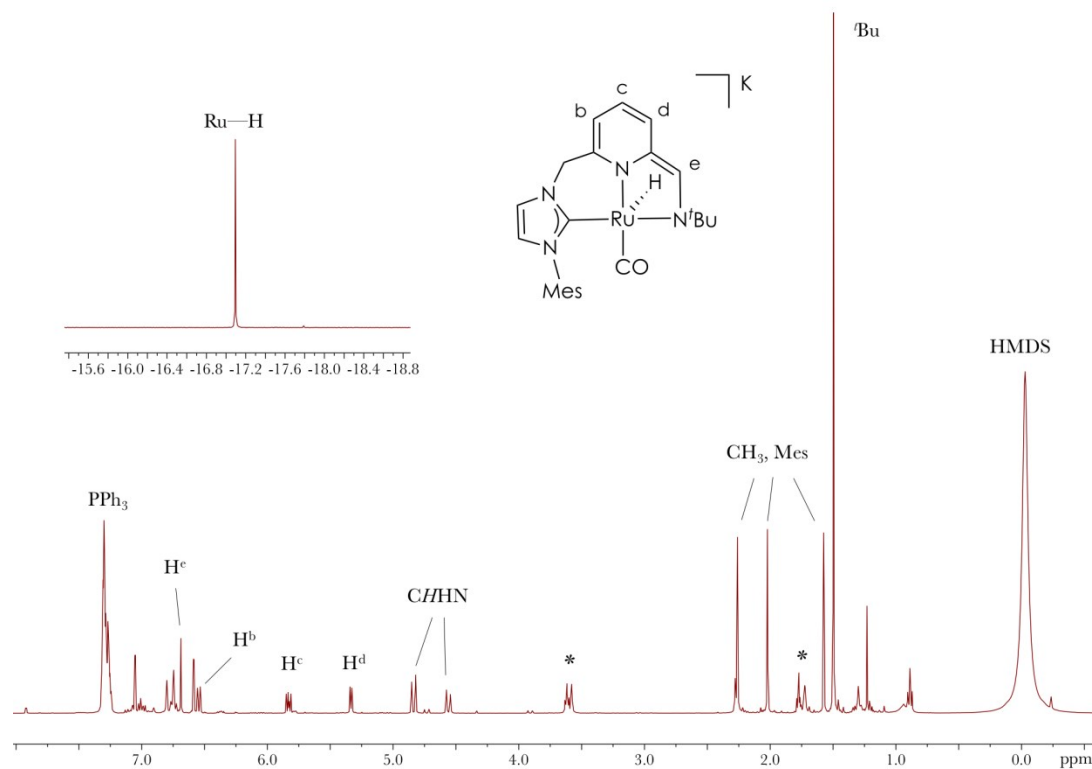


Figure S25. ^1H NMR spectrum (400 MHz) of the reaction of **3a** with KHMDS in $\text{THF-}d_8$ to yield **7** (* denotes residual THF).

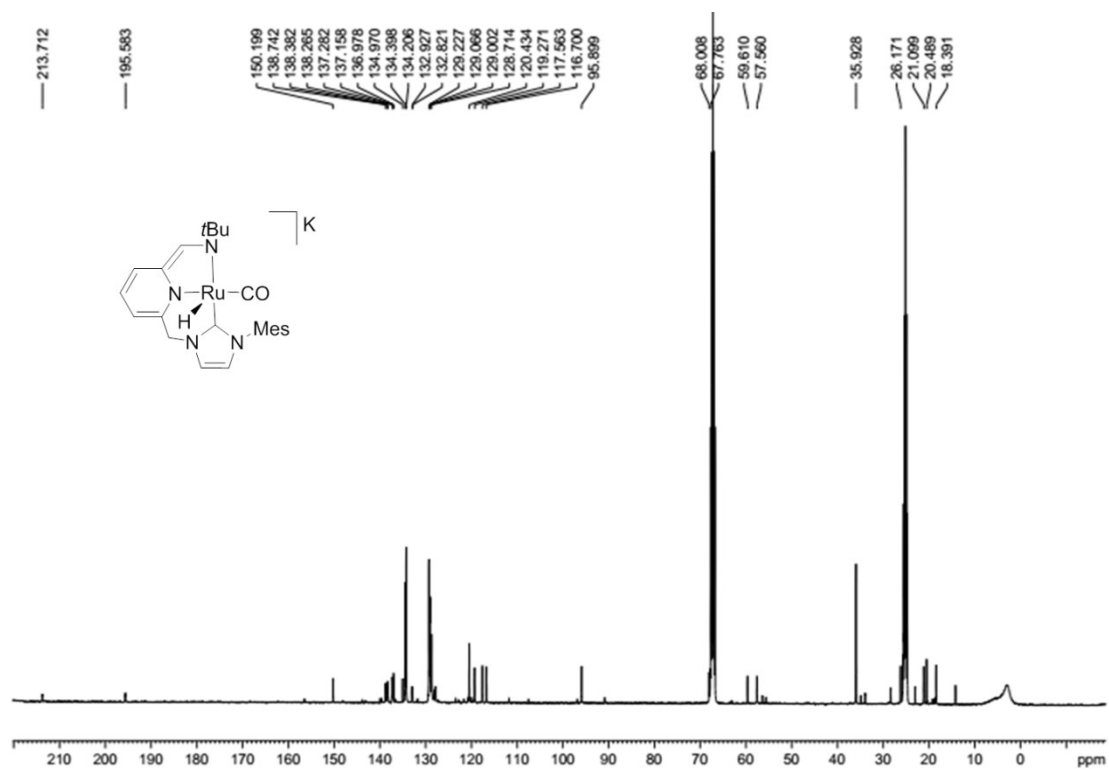


Figure S26. $^{13}\text{C}\{^1\text{H}\}$ NMR spectrum (101 MHz) of the reaction of **3a** with KHMDS in $\text{THF-}d_8$ to yield **7**.

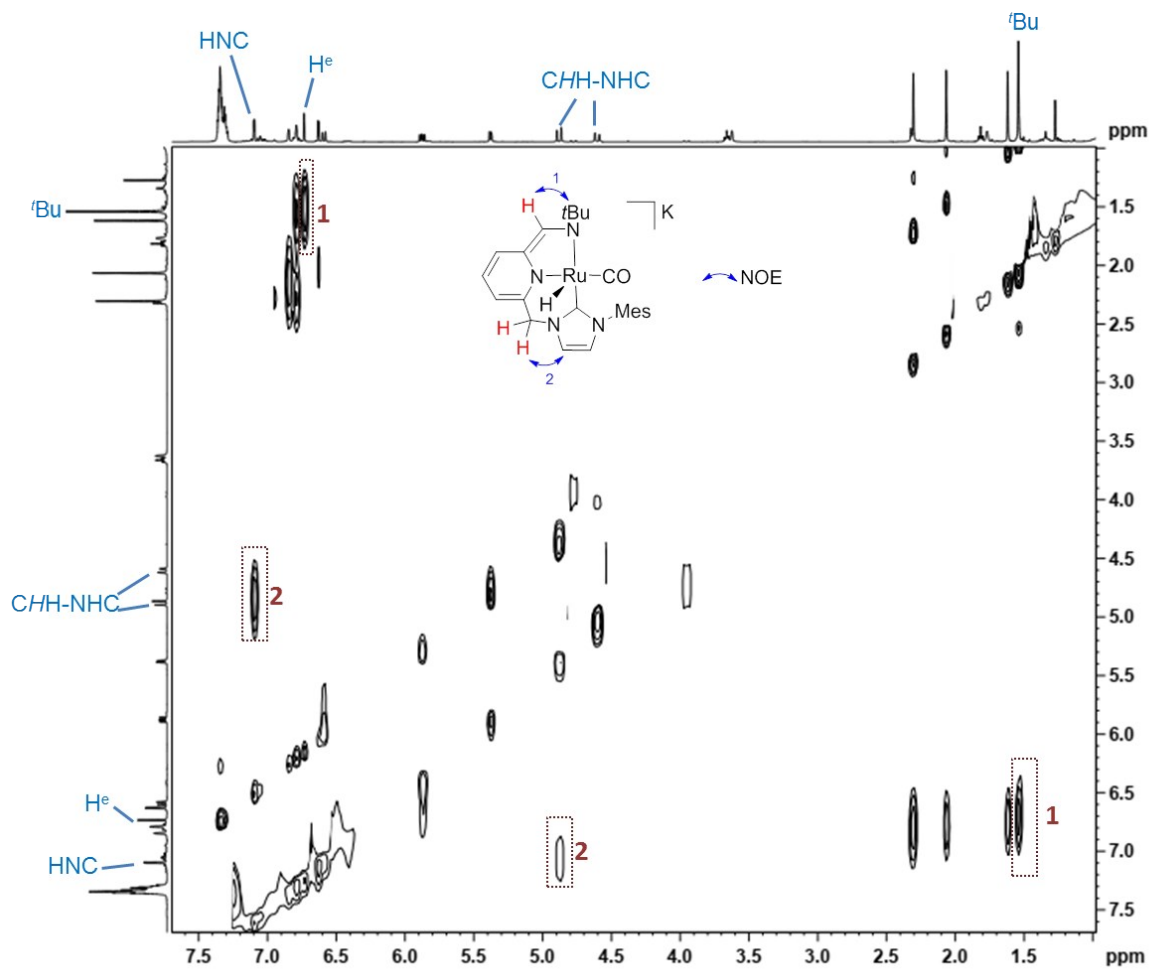


Figure S27. Selected region of the ^1H - ^1H NOESY spectrum (400 MHz) of the reaction of **3a** with KHMDS in THF- d_8 to yield **7**.

6.5. Selected NMR spectra for complex **8**

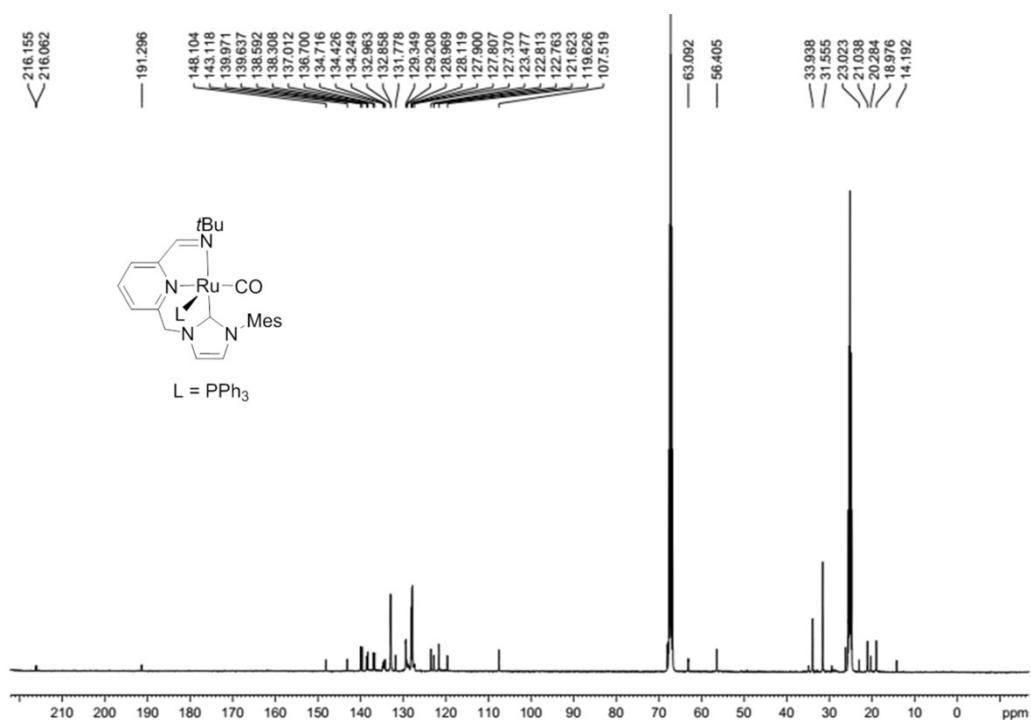
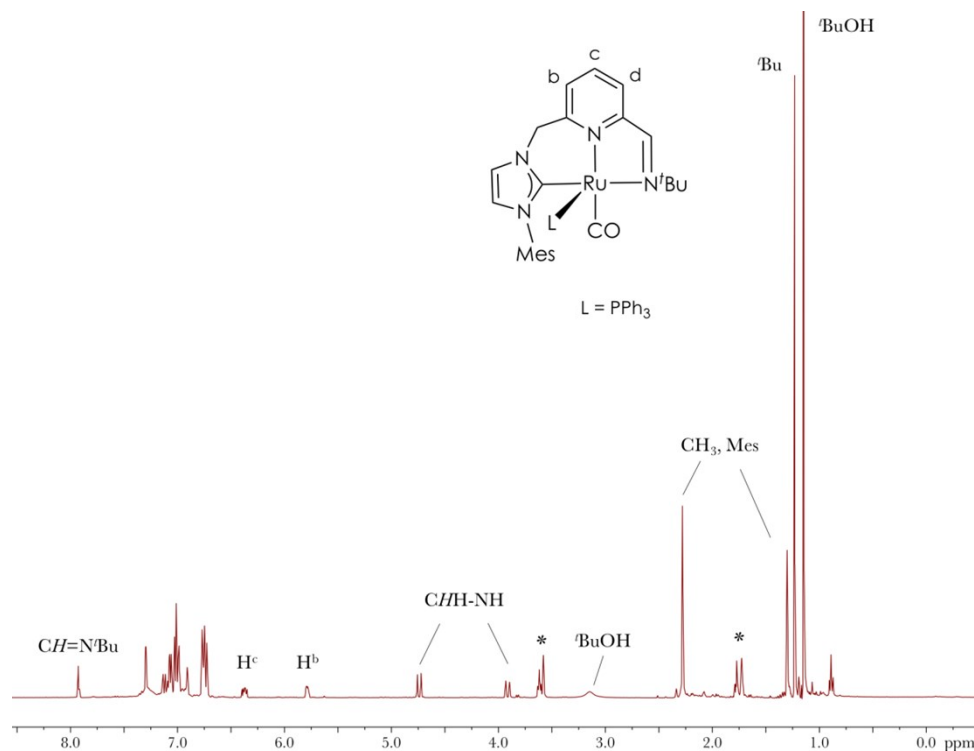


Figure S29. ¹³C{¹H} NMR spectrum (101 MHz) of the heated solution (60 °C) of the reaction of **3a** with KO^tBu in THF-*d*₈ to yield **8**.

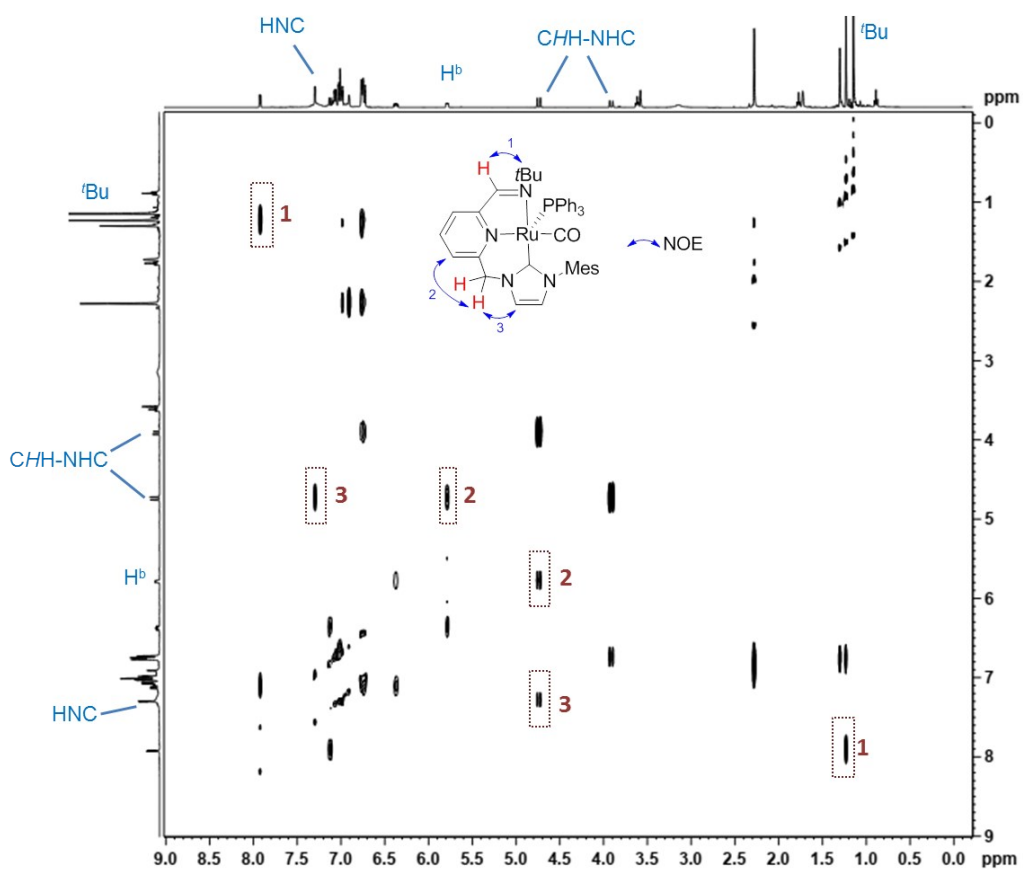


Figure S30. ^1H - ^1H NOESY spectrum (400 MHz) of the heated solution (60 °C) of the reaction of **3a** with KO^tBu in $\text{THF-}d_8$ to yield **8**.

7. NMR spectra of catalytic dehydrogenation reactions

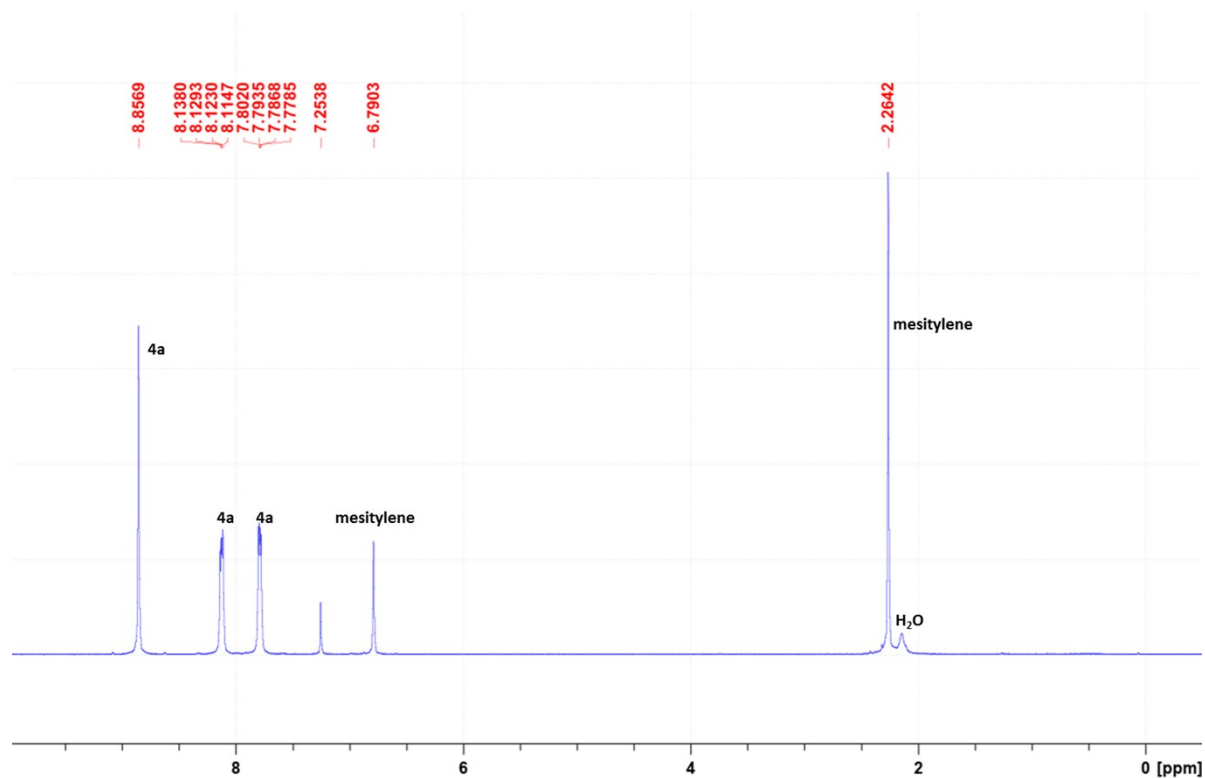


Figure S31. ¹H NMR spectrum (400 MHz, CDCl₃) of the dehydrogenation of 5a (Table 2, entry 1).

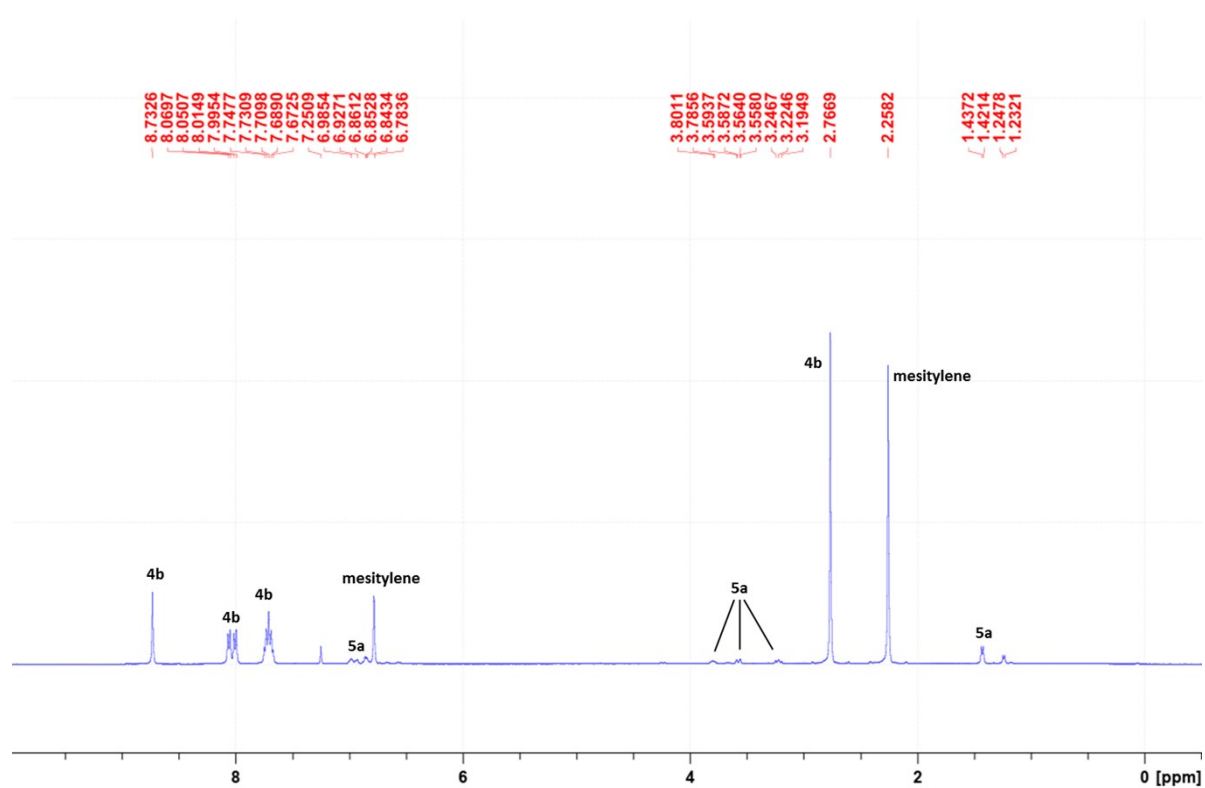


Figure S32. ¹H NMR spectrum (400 MHz, CDCl₃) of the dehydrogenation of 5b (Table 2, entry 2).

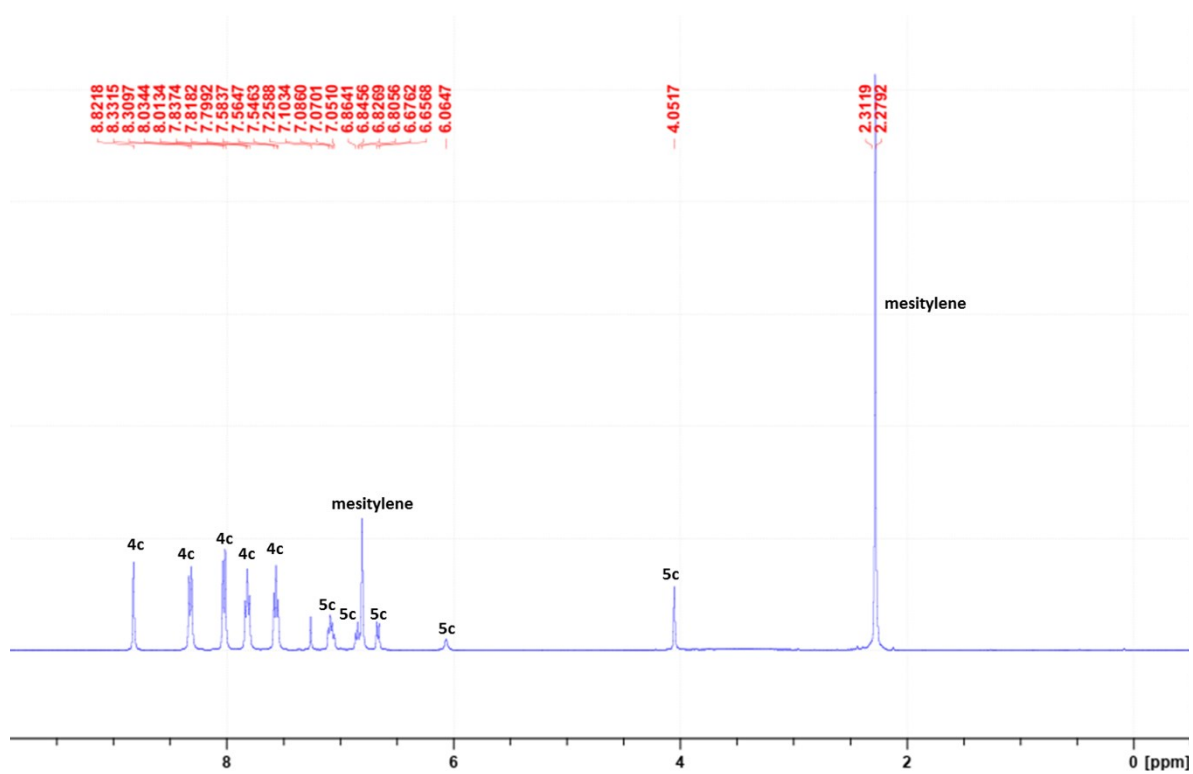


Figure S33. ^1H NMR spectrum (400 MHz, CDCl_3) of the dehydrogenation of **5c** (Table 2, entry 3).

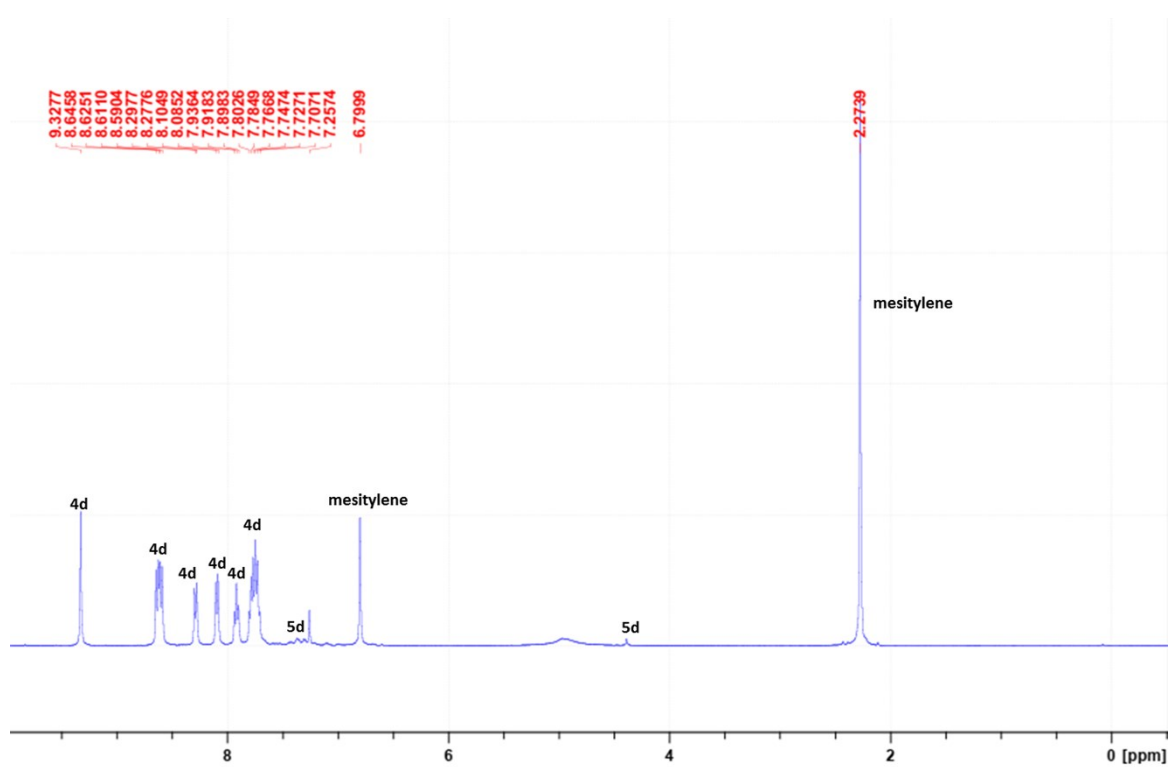


Figure S34. ^1H NMR spectrum (400 MHz, CDCl_3) of the dehydrogenation of **5d** (Table 2, entry 4).

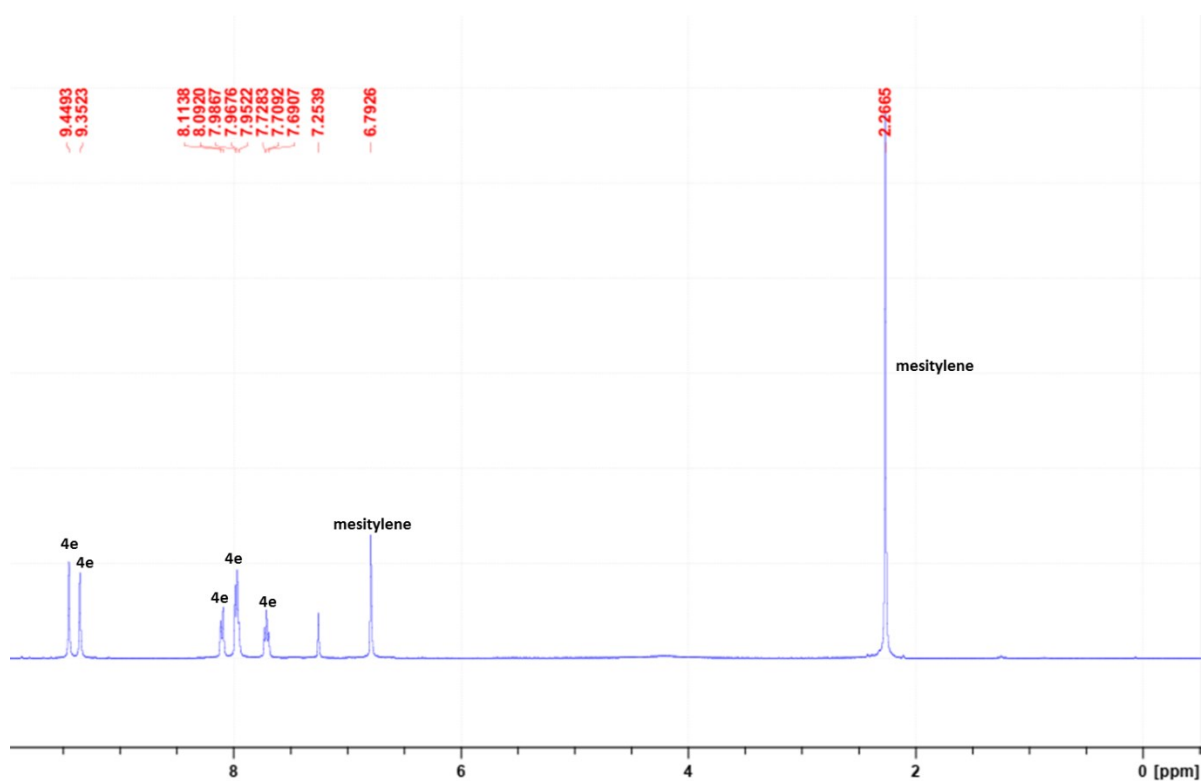


Figure S35. ^1H NMR spectrum (400 MHz, CDCl_3) of the dehydrogenation of **5e** (Table 2, entry 5).

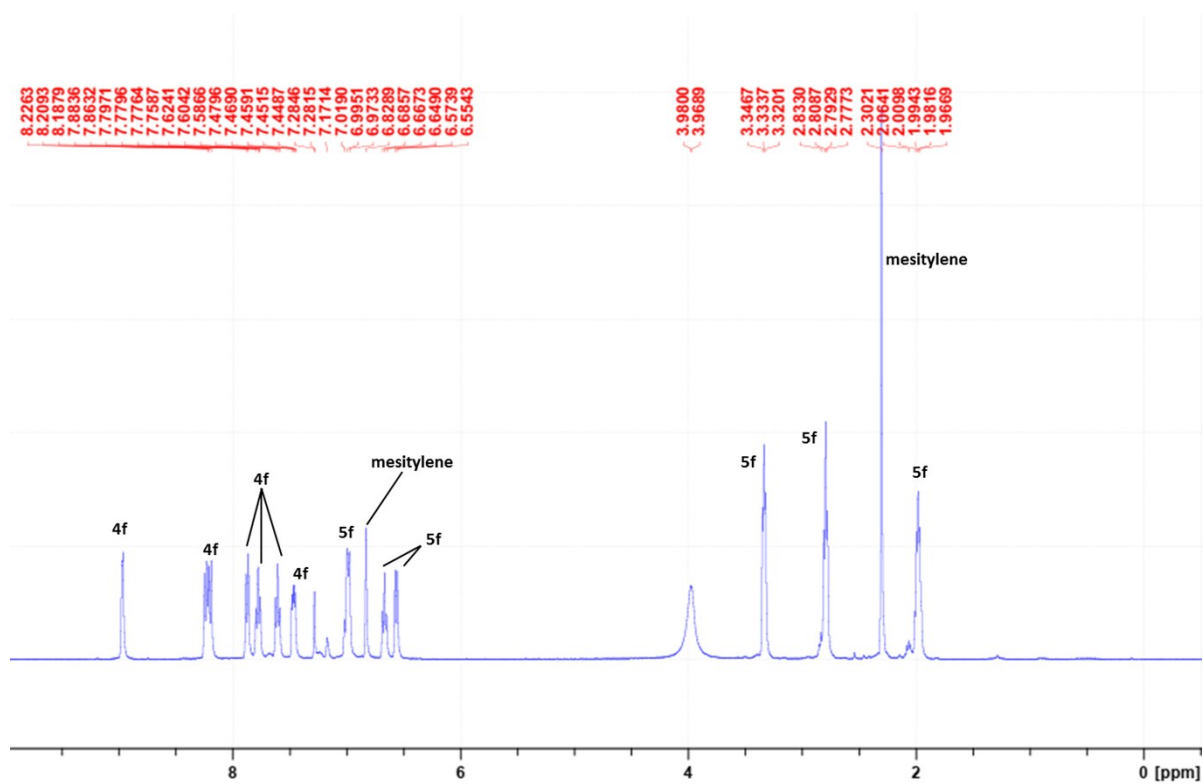


Figure S36. ^1H NMR spectrum (400 MHz, CDCl_3) of the dehydrogenation of **5f** (Table 2, entry 6).

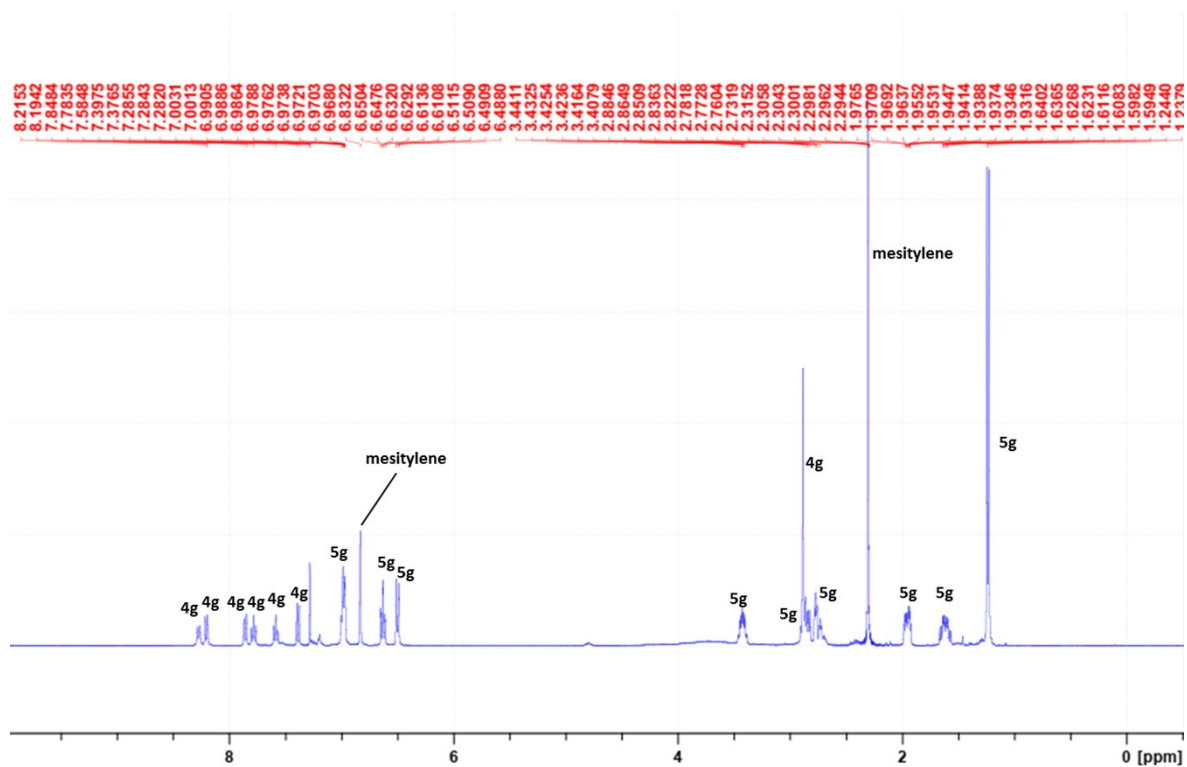


Figure S37. ^1H NMR spectrum (400 MHz, CDCl_3) of the dehydrogenation of **5g** (Table 2, entry 7).

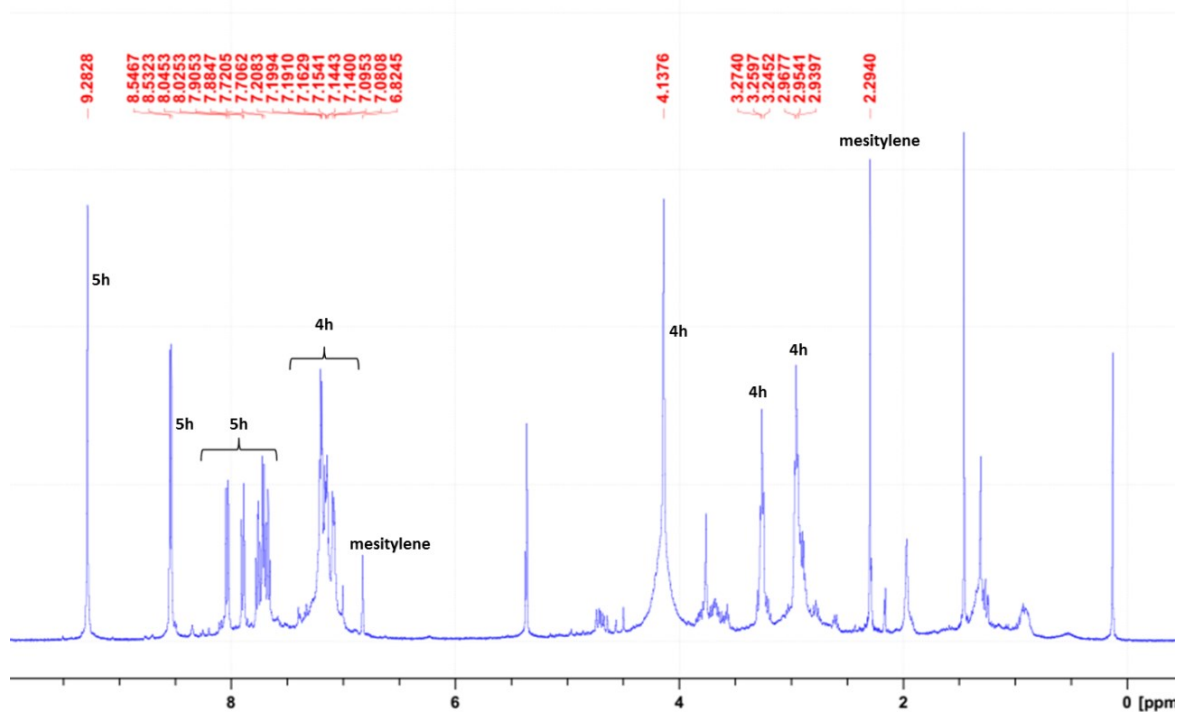


Figure S38. ^1H NMR spectrum (400 MHz, CD_2Cl_2) of the dehydrogenation of **5h** (Table 2, entry 8).

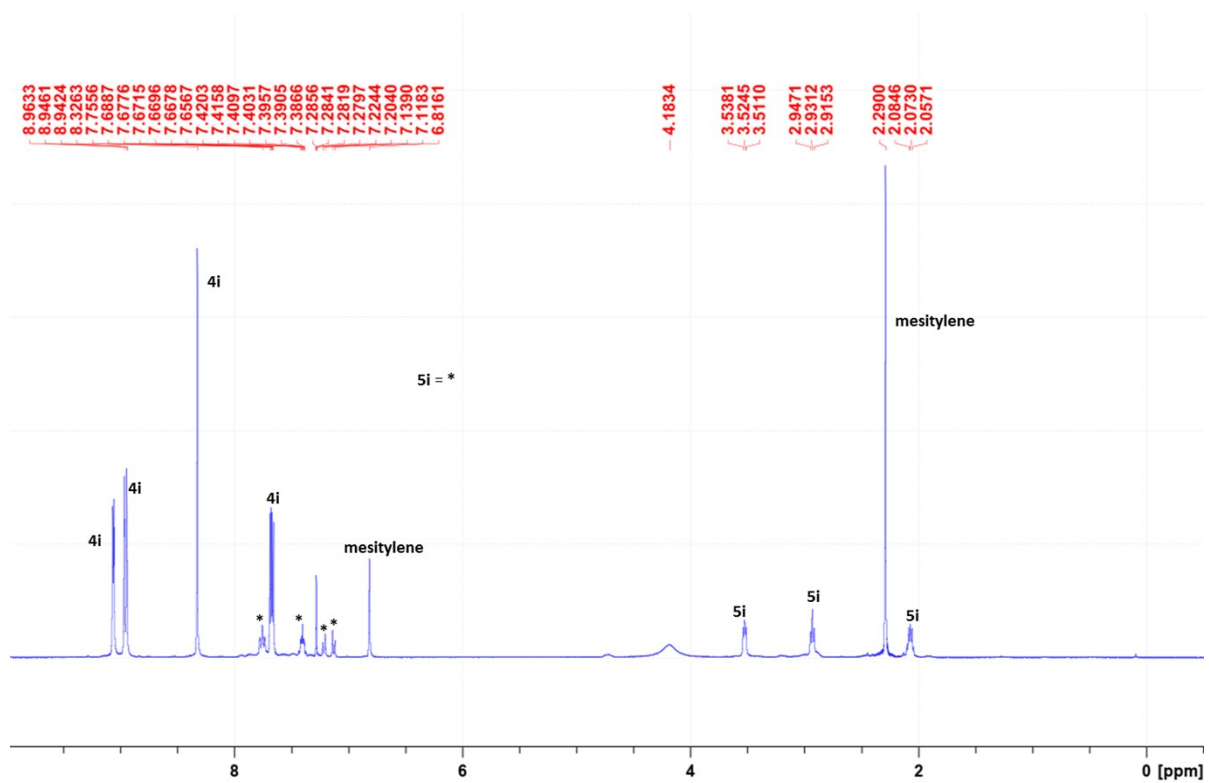


Figure S39. ^1H NMR spectrum (400 MHz, CDCl_3) of the dehydrogenation of **5i** (Table 2, entry 9).